Journal of Vertebrate Paleontology

Elasmosaurid phylogeny and paleobiogeography with a reappraisal of *Aphrosaurus furlongi* from the Maastrichtian of the Moreno Formation

J.P.O'Gorman[1,2]

[1]División Paleontología Vertebrados, Museo de La Plata, Universidad Nacional de La Plata, Paseo del Bosque s/n., B1900FWA, La Plata, Buenos Aires Province, Argentina.

[2] CONICET: Consejo Nacional de Investigaciones Científicas y Técnicas, Argentina.

joseogorman@fcnym.unlp.edu.ar

Supplementary Data 1

Table S1. Elasmosaurid OTU and hypodigms considered in this contribution. H = holotype. Specimens personally revised indicated by *.

OTU	Specimen
Aristonectes quiriquinensis	SGO PV 957 (H); SGO PV 260
Aristonectes parvidens	MLP 40-XI-14-6 (H*)
Albertonectes vanderveldei	TMP 2007.011.0001 (H*)
Alexandronectes zealandiensis	CM Zfr 73 (H*) (left part) + CM Zfr 91(H*) (right part)
Aphrosaurus furlong	LACM 2748 (H*)
Callawayasaurus colombiensis	UCPM 38349 (H*); (Bogota specimen: UCPM 125328*, skull and RA4425*, postcranium).
Elasmosaurus platyurus	ANSP 10081 (H*)
Eromangasaurus australis	QM F11050 (H)
Futabasaurus suzukii	NSM PV15025 (H)
Hydrotherosaurus alexandrae	UCMP 33912 (H*)
Kaiwhekea katiki	OU 12649 (H*)
Kawanectes lafquenianum	MLP 71-II-13-1 (H)*; MCS PV 4*; MUC Pv 92* and MPEF 1115
Libonectes morgani	SMUSMP 69120 (H); SMNK-PAL 3978 (H)
Morenosaurus stocki	LACM 2802 (H*)
Morturneria seymourensis	TTU P 9219 (H)
Nakonanectes bradti	MOR 3072 (H)
"Speeton Clay Plesiosaurian"	NHMUKR8623; SCARB200751*
Styxosaurus snowii	KUMNH 1301 (H)
Styxosaurus sp. *"Hydralmosaurus"*	AMNH 1495*+AMNH 5835*
Terminonatator ponteixensis	RSM P2414.1 (H)
Thalassomedon haningtoni	CMNH 1588 (H*)
Tuarangisaurus keyesi	NPC CD 425 and NPC CD 426 (H*)
Vegasaurus molyi	MLP 93-I-5-1 (H*)
Wapuskanectes betsynichollsae	TMP 98.49.02 (H*)
Zarafasaura oceanis	OCP DEK/GE 315 (H); OCP DEK/GE 456; WDC CMC-01.
Elasmosauridae indet.	LACM 2832

Institutional Abbreviations—**AMNH**: American Museum Natural History, New York, USA; **ANSP,** Academy of Natural Sciences of Philadelphia, USA; **CAMSM**, Sedgwick Museum of Earth Sciences, Cambridge, UK; **GPMM**, Geomuseum der Universität

Münster, Germany; **LACM**, Natural History Museum of Los Angeles County, Los Angeles Caunty, USA (previously housed on the **CIT**, California Institute of Technology, California, USA); **MANCH**, The Manchester Museum, Manchester, UK; **MCZ**, Museum of Comparative Zoology, Harvard University, Boston, USA; **MLP**, Museo de La Plata, Buenos Aires Province, Argentina; **NZGS**, Nuclear and Geological Science, Lower Hut, New Zealand; **MIWG**: 'Dinosaur Isle' Museum of Isle of Wight Geology, Sandown; **MNA**, Museum of Northern Arizona, Flagstaff, Arizona; **OXFUM**, Oxford University Museum of Natural History, Oxford; **QM**, Queensland Museum, Brisbane, Australia; **SGO PV**, Área Paleontologia, Museo Nacional de Historia Natural, Santiago de Chile, Chile; **TMP**, Tyrrell, Museum of Palaeontology, Drumheller, Alberta, Canada; **UCMP**, Museum of Paleontology, University of California, Berkeley, California, USA. **UNRN**, Universidad Nacional de Río Negro, Argentina.

Institutional Abbreviations—**fr**, frontal; **pa**, parietal.

Characters and scoring modifications

Characters 1-270 follow the numeration of Benson and Druckenmiller (2014), followed by Serratos et al. (2017), Sach and Kear, (2017) and mostly by Otero, 2016. Additional citations for each feature are given below. Character citation mostly based on Serratos et al. (2017) with some modifications.

Character modifications description

#*. Character name (*indicate that the character was modified). States (#) **Modification in black**.

OTU name

Ch # (**X**) S; (**Y**) O. Character number #, scored as "**X**" by Serratos et al. (2017) is scored as "**Y**" by O'Gorman in this contribution

All of the proposed changes are discussed in detail below to provide useful base for future phylogenetic and comparative studies.

Following Sachs et al. (2017) and Allemand et al. (2017) the scoring of *Libonectes morgani* and "*Libonectes atlasense*" where fused into a OTU. In the cases of different scores, characters were treated as polymorphic.

Ch. 2. Maxilla, lateral expansion of maxilla posterior to maxilla-premaxilla suture accommodates expanded caniniform bases ['roots']: absent (**0**); present (**1**). Benson et al. (2012a, Ch. 2). Modified from O'Keefe (2001, Ch. 9).

Callawayasaurus colombiensis

Ch. 2 (**0**) S; (**1**) O'G

Based on personal observation of UCPM 38349. The material shows different expansion in both sides probably due preservation.

15. Premaxilla contact along the dorsal midline: contacts anterior extension of frontals only (**0**); partially overlaps the frontal along the midline (**1**); overlaps the entire length of the frontal along the dorsal midline and contacts the parietal (**2**). Sato (2002, Ch. 6), Ketchum and Benson (2010, Ch. 10), Vincent et al. (2011, Ch. 5), Benson et al. (2012a, Ch. 14). Modified from Druckenmiller and Russell (2008, Ch. 5), O'Keefe (2001, Ch. 11), O'Keefe and Wahl (2003, Ch. 8),. State 1 from Bardet et al. (1999, Ch. 8), Smith and Dyke

(2008, Ch. 17), Modified from Großmann (2007, Ch. 6). State 2 from Carpenter (1999, Ch. 8).

Tuarangisaurus keyesi

Ch. 15 (**?**) S; (**2**) O'G

Based on personal observations and O'Gorman et al. (2017:fig. 7).

16. Premaxilla, posterior termination: tapering and non-interdigitating or weakly interdigitating (**0**); broad, deeply interdigitating suture with the frontal or parietal (**1**).

Sato (2002, Ch. 6), Benson et al. (2012b, Ch. 14). Modified from Benson et al. (2012a, Ch. 15).

Aristonectes parvidens

Ch. 16 (**0**) S; (**?**) O'G

This area is not preserved in the holotype and only specimen (MLP 40-XI-14-6) considered in this contribution (Gasparini et al., 2003:fig. 1; O'Gorman, 2016a:fig. 2.1, 2).

Callawayasaurus colombiensis

Ch. 16 (**?**) S; (**0**) O'G

Based on personal observation of the UCPM 38349 (Fig. S1A).

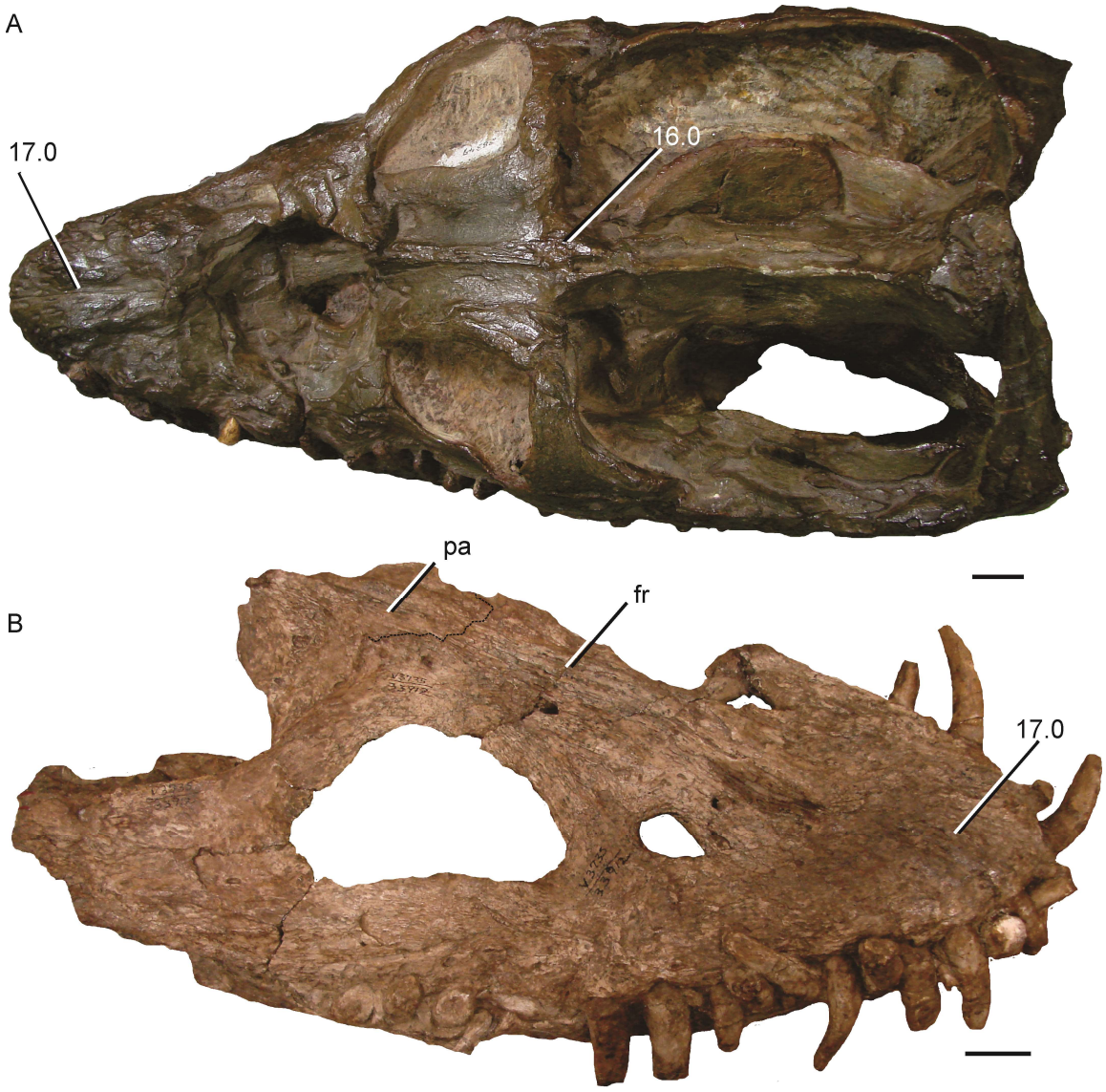

Fig. S1. **A**, *Callawayasaurus colombiensis* (UCPM 38349, holotype) in dorsal view. **B**, *Hydrotherosaurus alexandrae* (UCMP 33912, holotype). Scale bars equal 20 mm.

17. Premaxilla, dorsomedian ridge: absent or indistinct (**0**); prominent, forming eith1er a narrow crest, a broad bar-like ridge, or a mound-like eminence on the dorsomedian surface of the rostrum (**1**). Sato (2002, Ch. 3), Druckenmiller and Russell (2008, Ch. 6), Smith and Dyke (2008, Ch. 5), Ketchum and Benson (2010, Ch. 11), Benson et al. (2012a, Ch. 16).

Aristonectes parvidens

Ch. 17 (**1**) S; (**0**) O'G

Based on personal observation of MLP 40-XI-14-6 (Gasparini et al., 2003:fig 1).

Callawayasaurus colombiensis

Ch. 17 (**1**) S; (**0**) O'G

Based on personal observation of UCPM 38349 (Fig. S1A).

Hydrotherosaurus alexandrae

Ch. 17 (**1**) S; (**0**) O'G

Based on personal observation of UCMP 33912 (Fig. S1B).

Zarafasaura oceanis

Ch. 17 (**1**) S; (**?**) O'G

Based on Vincent et al., 2011:fig. 2A (OCP DEK/GE 315 seems to be deformed in this area) and Lomax and Wahl, 2013:fig. 5. Therefore it is not clear the state and therefore "?" is preferred.

18. Premaxilla, morphology of dorsomedian ridge: narrow and crest-like (taller than wide) (**0**); broad, occupying most of the internarial width of the rostrum (**1**); posterior mound (**2**). Modified from Ketchum and Benson (2010, Ch. 12), Benson et al. (2012a, Ch. 17) by addition of state 2 from Sato (2002, Ch. 10).

Callawayasaurus colombiensis

Ch. 18 (**0**) S; (**?**) O'G

Inapplicable character, based on scoring of Ch. 17.

Hydrotherosaurus alexandrae

Ch. 18 (0/2) S; (**?**) O'G

Inapplicable character, based on scoring of Ch. 17.

Zarafasaura oceanis

Ch. 18 (**0**) S; (**?**) O'G

Inapplicable character, based on scoring of Ch. 17

19. Premaxilla, dorsomedian ridge location: anterior (**0**); posterior (**1**); elongate, extends from interorbital region to rostral tip (**2**). Ketchum and Benson (2010, Ch. 13), Benson et al. (2012a, Ch. 18).

Callawayasaurus colombiensis

Ch. 19 (**1**) S; (**?**) O'G

Inapplicable character, based on scoring of Ch. 17.

Hydrotherosaurus alexandrae

Ch. 19 (**2**) S; (**?**) O'G

Inapplicable character, based on scoring of Ch. 17.

Zarafasaura oceanis

Ch. 19 (**2**) S; (**?**) O'G

Inapplicable character, based on scoring of Ch. 17.

22. Premaxilla, constriction of posteromedian process at level of external naris. absent (**0**); present, and does not expand to original width posterior to naris (**1**); present, but premaxilla expands to original width posterior to naris (**2**). Modified from Benson et al., 2012a, Ch. 21.

Aristonectes parvidens

Ch. 22 (**2**) S; (**?**) O'G

Based on personal observation of MLP 40-XI-14-6, the only specimen considered in this contribution (O'Gorman, 2016a:fig 2).

Kaiwhekea katiki

Ch. 22 (**2**) S; (**?**) O'G

The personal observation of the holotype indicted that this area is not well preserved and affected by a strong compression, therefore the scoring? is preferred.

35. Prefrontal participation in rim of external naris does not participate (**0**); participates (**1**).

O'Keefe (2001, Ch. 39), Sato (2002, Ch. 27), Druckenmiller and Russell (2008, Ch. 27), Smith and Dyke (2008, Ch. 16), Ketchum and Benson (2010, Ch. 25), Vincent et al. (2011, Ch. 4), Benson et al. (2012a, Ch. 31). Modified from Großmann (2007, Ch. 7).

Hydrotherosaurus alexandrae

Ch. 22 (**1**) S; (**?**) O'G

Based on personal observations it has not been possible to determine the state of this character.

36. Postfrontal participation in orbital margin participates (**0**); does not participate, excluded by postorbital-frontal contact (**1**).

O'Keefe (2001, Ch. 17); Sato (2002, Ch. 37), Druckenmiller and Russell (2008, Ch. 20), Ketchum and Benson (2010, Ch. 24), Vincent et al. (2011, Ch. 13).

Eromangasaurus australis

Ch. 36 (**0**) S; (**?**) O'G

Based on Kear 2005; 2007

41. Jugal-squamosal contact morphology: subvertical and interdigitating (**0**); subhorizontal for most of length, not interdigitating (**1**); inapplicable, contact absent (**?**).Benson and Druckenmiller, 2014 Ch. 41; Gasparini et al. (2003:fig. 3A), Vincent et al. (2011:fig. 2A–C).

Hydrotherosaurus alexandrae

Ch. 41 (**0**) S; (**?**) O'G

Based on personal observation, it was impossible to determined the suture in UCMP 33912 with certainty.

42. Postorbital-squamosal contact: present, excluding jugal from the margin of the supratemporal fenestra (**0**); absent, and jugal enters margin of the temporal fenestra (**1**). Carpenter (1999, Ch. 4), O'Keefe (2001, Ch. 28), Sato (2002, Ch. 15), O'Keefe and Wahl (2003, Ch. 18), Druckenmiller and Russell (2008, Ch. 21), Ketchum and Benson (2010, Ch. 31), Vincent et al. (2011, Ch. 15). Modified from Smith and Dyke (2008, Ch. 21).

Tuarangisaurus keyesi

Ch. 42 (**?**) S; (**0**) O'G.

Based on personal observations and O'Gorman et al., 2017.

43. Postorbital posterolateral process length: long, extending posteriorly for at least two-thirds of the temporal fenestra length (**0**); prominent, but not elongate, extending approximately one-third of temporal fenestra length (**1**); short or absent (**2**). Druckenmiller and Russell (2008, Ch. 22), Ketchum and Benson (2010, Ch. 33), Benson et al. (2012a, Ch. 35). Modified from Sato (2002, Ch. 38), Smith and Dyke (2008, Ch. 2). State 0 from

O'Keefe (2004*b*, Ch. 168), O'Keefe and Wahl (2003, Ch. 90), O'Keefe and Street (2009, Ch. 81). State 2 from from Bardet et al. (1999, Ch. 2), Gasparini et al. (2003, Ch. 2), Großmann (2007, Ch. 9).

Zarafasaura oceanis

Ch. 43 (**2**) S; (**1**) O'G.

Based on Vincent et al., 2011:fig. 2

44. Pineal foramen: present (**0**); absent (**1**). Carpenter (1997). Bardet et al. (1999, Ch. 10), Gasparini et al. (2003, Ch. 7), Albright et al. (2007, Ch. 6), O'Keefe (2008, Ch. 6), Vincent et al. (2011, Ch. 16). Modified from Druckenmiller and Russell (2008, Ch. 29), Ketchum and Benson (2010, Ch. 35).

Aristonectes parvidens

Ch. 44 (**0**) S; (**?**) O'G.

The area of the only specimen (40-XI-14-6, holotype) is not preserved in the *A. parvidens*.

Libonectes morgani

Ch. 44 (**1**) S; (**0**) O'G.

Base on the observations of Alleman et al., 2017.

***Styxosaurus* sp**. (AMNH 1495 and AMNH 5835).

Ch. 44 (**?**) S; (**1**) O'G.

Based on personal observation of the specimens AMNH 1495 and AMNH 5835

45. Pineal foramen, surrounding elements: enclosed entirely within the parietals (**0**); contacts the frontals or premaxillae anteriorly (**1**); inapplicable, pineal foramen absent (**?**). O'Keefe (2001, Ch. 21), O'Keefe and Wahl (2003, Ch. 31), Druckenmiller and Russell

(2008, Ch. 30), Smith and Dyke (2008, Ch. 26), O'Keefe and Street (2009, Ch. 13), Ketchum and Benson (2010, Ch. 36), Vincent et al et al. (2011, Ch. 17), Benson et al et al. (2012a, Ch. 36). Serratos et al., 2017; Benson and Druckenmiller, 2014. Modified from Sato (2002, Chs 29 and 32).

Aristonectes parvidens

Ch. 45 (**1**) S; (**?**) O'G.

This area is not preserved in the *A*. *parvidens* holotype and only specimen (40-XI-14-6, holotype).

46. Pineal foramen-location relative to postorbital bar: level with postorbital bar (**0**); just posterior to postorbital bar (**1**). inapplicable, pineal foramen absent (**?**).

Benson and Druckenmiller, 2014.

Aristonectes parvidens

Ch. 45 (**0**) S; (**?**) O'G.

This area is not preserved in the *A*. *parvidens* holotype and only specimen (40-XI-14-6, holotype).

Eromangasaurus australis

Ch. 45 (**1**) S; (**?**) O'G.

The holotype of *E*. *australis* (QM F11050) is so crushed (Kear, 2005, 2007) that this type of characters, is almost impossible to score with certainty.

47. Morphology of pineal foramen: suboval (**0**); anteroposteriorly elongate and slot-like (**1**); inapplicable, pineal foramen absent (**?**). Benson and Druckenmiller, 2014.

Aristonectes parvidens

Ch. 47(**1**) S; (**?**) O'G.

This area is not preserved in the *A. parvidens* holotype and only specimen (40-XI-14-6, holotype).

Eromangasaurus australis

Ch. 47(**0**) S; (**?**) O'G.

The holotype of *Eromangasaurus australis* (QM F11050) is so crushed that this type of characters, is almost impossible to score with certainty.

50. Parietal, sagittal crest height: crest absent, dorsal surface of parietal broad and flat (**0**); low, transversely convex (**1**); high, transversely compressed sheet (**2**); very high, forming convex dome in lateral view rising above the skull table (**3**). Benson et al et al. (2012a, Ch. 39); Modified from O'Keefe and Wahl (2003, Ch. 94), O'Keefe (2008, Ch. 32), O'Keefe and Street (2009, Ch. 85), Benson et al et al. (2012b, Ch. 182).

Aristonectes parvidens

Ch. 47 (**3**) S; (**?**) O'G.

The parietal table is not preserved in the *A. parvidens* holotype and only specimen (40-XI-14-6, holotype).

Aristonectes quiriquinensis

Ch. 47 (**3**) S; (**?**) O'G.

The parietal table is not well preserved in the holotype, SGO PV 957.

52. Parietal, anterior extension: short or absent, parietal extends to the level of the temporal bar (**0**); long, parietal extends to orbital midlength or more anteriorly (**1**); very

long, parietal extends to anterior orbit margin or more anteriorly (**2**). Benson et al. (2012b, Ch. 181), Benson et al. (2012a, Ch. 41).

Aristonectes parvidens

Ch. 52 (**1**) S; (**?**) O'G.

The parietal of the only specimen (40-XI-14-6, holotype) is not preserved in the *A. parvidens*.

Tuarangisaurus keyesi

Ch. 52 (**?**) S; (**?**) O'G.

Based on O'Gorman et al. (2017).

53*. Squamosal arch, posterior margin in dorsal view: dorsal processes extend anterolaterally (**0**); approximately straight, squamosal dorsal processes extend laterally from midline contact (**1**); V-shaped, squamosal dorsal processes extend posterolaterally (**2**); **Very deep v shaped notch formed by squamosals extending anteriorly beyond the level of the foramen magnum in dorsal view (3)**. Modified from Benson and Druckenmiller, 2014, by adding state (3)

Aristonectes quiriquinensis Ch. 53 (**2**) S; (**3**) O'G ***/Zarafasaura oceanis*** Ch. 53 (**2**) S; (**3**) O'G

Based on definition of state 3 and Otero et al. (2018) and Lomax and Wahal (2013).

Aristonectes parvides

Ch. 53 (**2**) S; (**?**) O'G.

This area is not preserved in the *A. parvidens* holotype and only specimen (40-XI-14-6, holotype).

Eromangasaurus australis

Ch. 53 (**?**) S; (**1**) O'G.

Based on Kear (2007: fig 1).

56. Temporal bar, dorsoventral thickness: low, significantly less than height of orbit (**0**); high, subequal to 2/3 or greater than height of orbit (**1**). Modified from O'Keefe (2008, Ch. 40).

Hydrotherosaurus alexandrae

Ch. 56(**1**) S; (**?**) O'G.

A personal observation of the holotype UCPM 33912 does not allows determining the state with certainty.

58. Inter-squamosal suture along the posterodorsal midline: flat (**0**); prominent, 'bulb-like' posterior extension (**1**); low, mediolaterally broad posterior convexity in dorsal view (**2**). Modified from O'Keefe (2001, Ch. 55), Sato (2002, Ch. 72), Druckenmiller and Russell (2008, Ch. 34), Smith and Dyke (2008, Ch. 30), Ketchum and Benson (2010, Ch. 42), Benson et al. (2012a, Ch. 43) by addition of state 2.

Aristonectes parvidens

Ch. 58 (**0**) S; (**?**) O'G.

The area of the only specimen (MLP 40-XI-14-6, holotype) is not preserved in the *A. parvidens*.

Hydrotherosaurus alexandrae

Ch. 58 (**1**) S; (**?**) O'G.

A personal observation of the holotype UCPM 33912 does not allow determining the state with certainty.

Thalassiodracon hawkinsii

Ch. 58 (**1**) S; (0/1) O'G.

Based on personal observation of CAMSM J.46986 (SFig, 2.A) and Benson et al., 2011:fig. 1C. The character seems to be polymorphic.

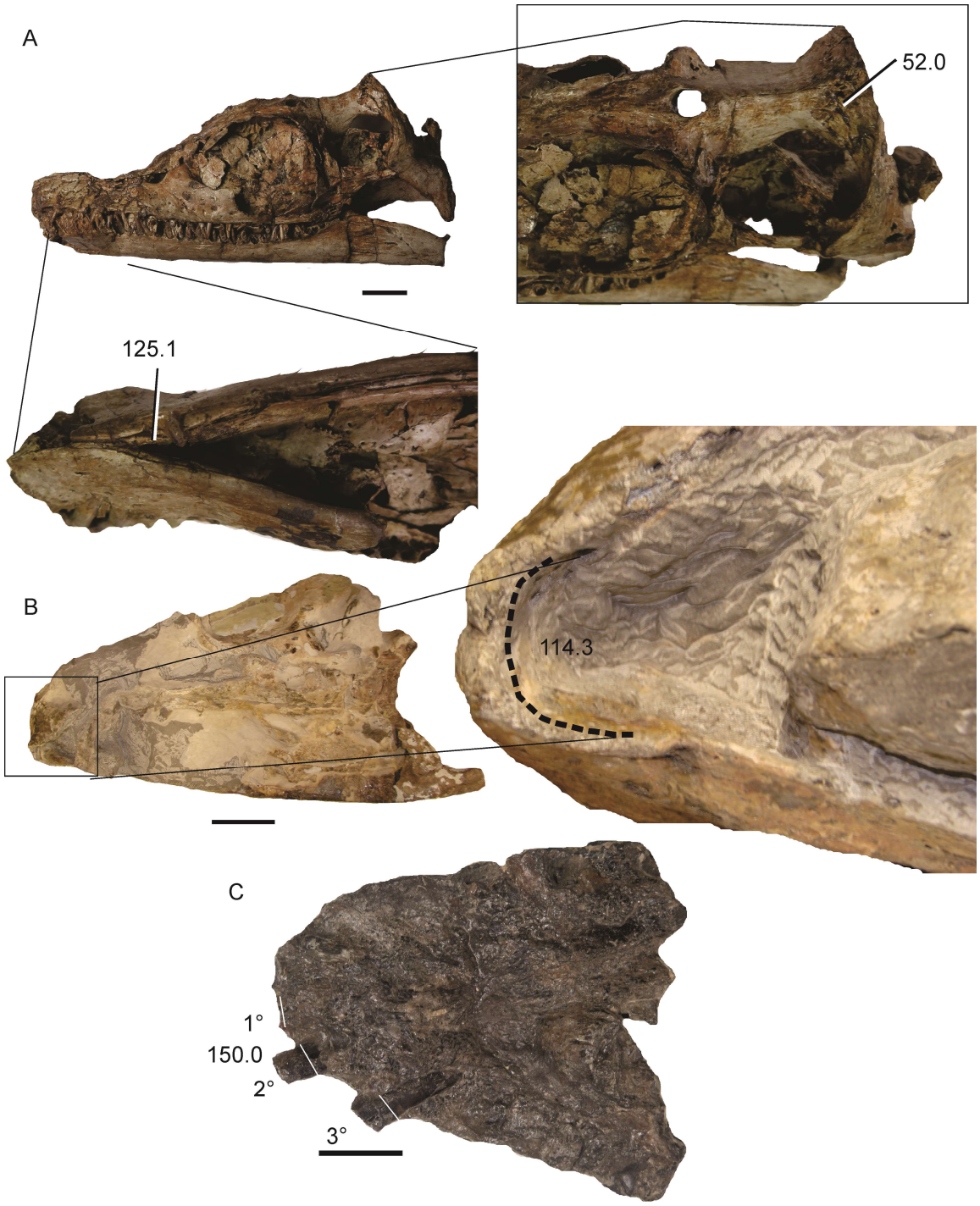

FIGURE S2. **A**, *Thalassiodracon hawkinsii* (CAMSM J.46986) skull in left lateral view and details of symphysis and squamosal. Scale bar equals 20 mm. **B**, *Kaiwhekea katiki* (OU

12649) skull in ventral view. Scale bar equals 100 mm. **C**, *Elasmosaurus platyurus* (ANSP 10081), premaxilla in ventral view. Scale bars equal 20 mm.

61. Squamosal, outline of posterior margin in lateral view: approximately straight (**0**); dorsal portion inflected abruptly anterodorsally (**1**).

Benson et al. (2012a, Ch. 46).

Hydrotherosaurus alexandrae

Ch. 61 (**0**) S; (**?**) O'G.

A personal observation of UCPM 33912 (holotype) does not allow determining the state with certainty.

Kaiwhekea katiki

Ch. 61 (**0**) S; (**?**) O'G.

A personal observation of OU 22344 (holotype) does not allow determining the state with certainty.

62. Position of tooth row in lateral view: collinear with the mandibular glenoid fossa (**0**); considerably higher than the glenoid fossa (**1**). O'Keefe (2001, Ch. 98), Sato (2002, Ch. 91), Gasparini et al et al. (2003, Ch. 11), O'Keefe and Wahl (2003, Ch. 53), Druckenmiller and Russell (2008, Ch. 82), O'Keefe and Street (2009, Ch. 44), Ketchum and Benson (2010, Ch. 94), Vincent et al. (2011, Ch. 41), Benson et al. (2012a, Ch. 47).

After a comparison and revision of available material and figures no marked differences in this character was observed among elamosaurids. Therefore all were scored as "0".

Probably little differences are present but the deformation by dorsoventrally crushing

usually generate that the original differences remains obscured and be source of non-taxonomic information.

63. Notochordal pit on occipital condyle: absent (0); present (1).

65. Occipital condyle constriction: complete, exoccipital facets are separated from the occipital condyle by a groove (**0**); incomplete because exoccipital facets contact the occipital condyle (**1**); or constricting groove altogether absent, even ventrally (**2**). Sato (2002, Ch. 78), Druckenmiller and Russell (2008, Ch. 69), Benson et al. (2012a, Ch. 49). Modified from Bardet et al. (1999, Ch. 14), O'Keefe (2001, Ch. s 42 and 43), Gasparini et al. (2002, Ch. 7), Sato (2002, Ch. 77), O'Keefe and Wahl (2003, Ch.s 22 and 23), Druckenmiller and Russell (2008, Ch. 68), O'Keefe and Street (2009, Chs 19 and 20), Ketchum and Benson (2010, Ch. 79), Vincent et al. (2011, Ch. 33).

Aristonectes parvidens

Ch. 65 (**1**) S; (**?**) O'G.

The material is not available for revision and the original description of Cabrera (1941) does not allow to be sure about the state.

67. Foramen magnum, proportion of foramen enclosed by supraoccipital: less than one-third (**0**); approximately half (**1**).

Benson and Druckenmiller (2014, Ch. 67).

Aristonectes parvidens

Ch. 67 (**0**) S; (**?**) O'G.

This area is not preserved in the *A. parvidens* holotype and only specimen (40-XI-14-6, holotype).

71. Opisthotic, orientation of paraoccipital process relative to ventral surface of exoccipital in posterior view: inclined dorsally (**0**); paraoccipital process oriented parallel to ventral surface of exoccipital (**1**); inclined ventrally (**2**).

Benson et al. (2012a, Ch. 54). Modified from O'Keefe (2001, Ch. 48), Sato (2002, Ch. 67), O'Keefe and Wahl (2003, Ch. 26), Großmann (2007, Ch. 22), Druckenmiller and Russell (2008, Ch. 65), O'Keefe and Street (2009, Ch. 22), Ketchum and Benson (2010, Ch. 77).

Aristonectes parvidens

Ch. 71 (**2**) S; (**?**) O'G.

This area is not preserved in the *A. parvidens* holotype and only specimen (40-XI-14-6, holotype).

72. Opisthotic, morphology of articulation with suspensorium (paraoccipital process): anterior surface of expanded lateral end makes broad contact with suspensorium (**0**); lateral end unexpanded, lateral/terminal surface makes narrow contact with suspensorium (**1**).

Benson et al. (2012a, Ch. 55). Modified from O'Keefe (2001, Ch. 49), O'Keefe and Wahl (2003, Ch. 27).

Aristonectes parvidens

Ch. 72 (**0**) S; (**?**) O'G.

This area is not preserved in the *A. parvidens* holotype and only specimen (40-XI-14-6, holotype).

Aristonectes quiriquinensis

Ch. 72 (**0**) S; (**1**) O'G.

The area of the only specimen MLP 40-XI-14-6 (holotype) is not preserved in the *A. parvidens*.

Libonectes morgani

Ch. 72(**?**) S; (**0**) O'G.

Based on Carpenter, 1999:fig. 2B.

Tuarangisaurus keyesi

Ch. 72 (**?**) S; (**1**) O'G.

Although some uncertainty exists as the distalmost tip of the paraoccipital process not preserved the observation of NPC CD 425 indicate this scoring. The CM Zfr 115 recently referred to the same genus reinforces this assumption (O'Gorman, 2017:fig. 9A, B; Hiller et al., 2017:fig. 6j).

83. Parasphenoid (or parabasisphenoid), morphology of ventral surface within interpterygoid vacuity: mediolaterally concave (**0**); flat or weakly convex (**1**); bears distinct midline keel (**2**); inapplicable, parasphenoid does not extend far into posterior interpterygoid vacuity (**?**). Benson et al. (2012a, Ch. 63). Modified from Ketchum and Benson (2010, Ch. 68). States 1 and 2 from O'Keefe (2008, Ch. 43). State 2 from O'Keefe (2001, Ch. 71), Sato (2002, Ch. 61), Druckenmiller and Russell (2008, Ch. 55), Smith and Dyke (2008, Ch. 48), Vincent et al. (2011, Ch. 25).

Tuarangisaurus keyesi

Ch. 83 (**?**) S; (**2**) O'G.

Based on personal observation and O'Gorman et al. (2017:fig. 9F, I).

92. Pterygoid-vomer contact: pterygoid does not separate vomers along midline (0); pterygoid separates vomers along the midline posteriorly (1). Ketchum and Benson (2010, Ch. 54), Vincent *et al.* (2011, Ch. 22), Benson *et al.* (2012*a*, Ch. 71).

Tuarangisaurus keyesi

Ch. 92 (**?**) S; (**0**) O'G.

Based on O′Gorman et al., 2017. The segmentation shows a small posterior notch, however this is shallow and seems to be due poor preservation of the posterior mart of the vomer.

99. Pterygoids, midline contact posterior to posterior interpterygoid vacuity: absent (**0**); present posteriorly, but very small (**1**); present, pterygoid contact for more than two-thirds of their anteroposterior length posterior to posterior interpterygoid vacuity (**2**). Sato (2002, Ch. 50), Benson et al. (2012a, Ch. 76). Modified from Bardet et al. (1999, Ch. 12), Carpenter (1999, Ch. 3), O'Keefe (2001, Ch. 62), O'Keefe and Wahl (2003, Ch. 35), Großmann (2007, Ch. 19), O'Keefe (2008, Ch. 44), Druckenmiller and Russell (2008, Ch. 50), Smith and Dyke (2008, Ch. 44), O'Keefe and Street (2009, Ch. 26), Ketchum and Benson (2010, Ch. 63), Vincent et al. (2011, Ch. 27).

Aristonectes quiriquinensis

Ch. 99 (**?**) S; (**0**) O'G.

Based on Otero et al. (2016) and Otero et al. (2018:fig. 4).

Tuarangisaurus keyesi

Ch. 99 (**2**) S; (**0**) O'G.

O'Gorman et al. (2017) redescribe the *Tuarangisaurus keyesi* holotype and O'Gorman et al., (2018) pointed the possibility of absence of posterior interpterygoid symphysis. A reexamination of the CT scans of *T. keyesi* shows that it probably lacks a posterior interpterygoid symphysis as no remains of pterygoid is attached below the basisphenoid or basioccipital and therefore it is score as "0"

102. Pterygoid, posterolateral portion of pterygoid: does not form squared lappet (**0**); forms squared lappet that distinctly underlaps quadrate ramus of pterygoid (**1**). O'Keefe (2001, Ch. 58), O'Keefe and Wahl (2003, Ch. 33), Druckenmiller and Russell (2008, Ch. 57), Smith and Dyke (2008, Ch. 46), O'Keefe and Street (2009, Ch. 24), Ketchum and Benson (2010, Ch. 66), Benson et al. (2012a, Ch. 79).

Aristonectes quiriquinensis

Ch. 102 (**1**) S; (**0**) O'G.

Kaiwhekea katiki

Ch. 102 (**?**) S; (**0**) O'G.

109. Ectopterygoid/pterygoid boss/flange: absent (**0**); ventrally deflected posterior margin forms flange (**1**); rugose ventral boss present (**2**). Benson et al. (2012a, Ch. 84). Modified from O'Keefe (2001, Ch. 84), Sato (2002, Ch. 57), Druckenmiller and Russell (2008, Ch. 47), Ketchum and Benson (2010, Ch. 58). Modified from Sato (2002, Ch. 56).

Tuarangisaurus keyesi

Ch. 109 (**?**) S; (**2**) O'G

Based on O'Gorman et al., 2017:fig. 7B

110*. Ectopterygoid/pterygoid boss, transverse width: approximately as wide mediolaterally as long anteroposteriorly (**0**); >1.5 times as wide mediolaterally as long anteroposteriorly (**1**).

Modified from Benson and Druckenmiller, 2014 by addition of state 2.

Tuarangisaurus keyesi

Ch. 110 (**?**) S; (**1**) O'G.

Based on O'Gorman et al., 2017:fig. 8E, D.

111. Shape of the mandible seen in dorsal/ventral view: bowed medially anterior to glenoid (**0**); not significantly bowed (**1**). Sato (2002, Ch. 85), Druckenmiller and Russell (2008, Ch. 75), Smith and Dyke (2008, Ch. 60), Ketchum and Benson (2010, Ch. 86), Vincent et al. (2011, Ch. 35), Benson et al. (2012a, Ch. 86). Modified from O'Keefe (2001, Ch. 86).

This character is difficult to score due the subjectivity; however a single criterion was followed and only the strongly bowed mandibles are scored as "0".

Eromangasaurus australis

Ch. 111 (**?**) S; (**1**) O'G.

Kaiwhekea katiki

Ch. 111 (**0**) S; (**?**) O'G.

Based comparison and personal observation of OU 12649.

Libonectes morgani

Ch. 111 (**0**) S; (**1**) O'G.

Based on Carpenter (1999:fig 2E).

Zarafasaura oceanis

Ch. 111 (**0**) S; (**1**) O'G.

Based comparison in Vincent et al. (2011:fig 4, 5).

112*. Mandible, symphysis length as measured by the number of alveoli adjacent to the symphysis [relative to the number of maxillary teeth or an estimate thereof]: long symphysis, number of alveoli adjacent to symphysis equals 0.4–0.5 of maxillary alveolar count (**0**); intermediate, 0.20–0.30 (**1**); **< 0.20** (**2**). Benson et al. (2012a, Ch. 87). Modified from Sato (2002, Ch. 87), Albright et al. (2007, Ch. 8), Druckenmiller and Russell (2008, Ch. 79), O'Keefe (2008, Ch. 8), Smith and Dyke (2008, Ch. 54), Ketchum and Benson (2010, Ch. 113), Vincent et al. (2011, Ch. 36) (different quantification). Modified from O'Keefe (2001, Ch. 89), O'Keefe and Wahl (2003, Ch. 48), O'Keefe and Street (2009, Ch. 39): lateral expansion of the mandibular symphysis is coded separately here (Ch. 113). Modified from Serratos et al 2017.

Aristonectes parvidens

Ch. 112 (**1**) S; (**2**) O'G based on personal observation of MLP 40-XI-14-6 (holotype).

Aristonectes quiriquinensis

Ch. 112 (**1**) S; (**2**) O'G

Based on Otero et al., 2014.

Kaiwhekea katiki

Ch. 112 (**1**) S; (**2**) O'G

Based on personal observations of OU 12649 (holotype, Sfig 2B).

Kawanectes lafquenianum

Ch. 112 (**?**) S; (**2**) O'G.

Based on O'Gorman, 2017.

114*. Structure of the dentary along the ventral surface of the mandibular symphysis: no ventral elaboration (**0**); forms raised ventral platform or sharp keel/ridge adjacent to symphysis (**1**); forms an anteroposterior narrow sulcus (**2**). **broad sulcus** (**3**). Modified from Benson and Druckenmiller, 2014 by addition of state 3. Modified for O'Keefe (2001, Ch. 88), Smith and Dyke (2008, Ch. 57), Vincent et al. (2011, Ch. 38). Druckenmiller and Russell (2008, Ch. 80), Ketchum and Benson (2010, Ch. 92); Modified from Benson et al. (2012a, Ch. 89).

Aristonectes parvidens

Ch. 114 (**1**) S; (3) O'G. Based on personal observation of MLP 40-XI-14-6. See O'Gorman, (2016a:fig. 4.1).

Aristonectes quiriquinensis

Ch. 114 (**1**) S; (3) O'G.

Based on Otero (2014:fig. 8B).

Kaiwhekea katiki

Ch. 114 (**1**) S; (3) O'G.

Based on personal observation on OU 12649 (holotype) see SFig 2B.

Kawanectes lafquenianum

Ch. 114 (**?**) S; (**2**) O'G

Based on personal observation of the referred specimen MPEF 115

Libonectes atlasense

Ch. 114 (**0**) S; (**1**) O'G

Based on Sach and Kear, 2017.

Tuarangisaurus keyesi

Ch. 114 (**?**) S; (**2**) O'G

Based on O′Gorman et al., 2017: fig: 9L.

122. Mandible, retroarticular process, dorsoventral orientation of long axis: posterodorsal (0); posteroventral or subhorizontal (1). Benson *et al.* (2012*a*, Ch. 94).

Kawanectes lafquenianum

Ch. 122 (**?**) S; (**1**) O'G

Based on personal observation of the referred specimen MPEF 115

123. Mandible, retroarticular process, mediolateral orientation of long axis: directly posterior, in line with 'anteroposterior' long axis of glenoid (0); inflected slightly posteromedially (1).

Benson *et al.* (2012*a*, Ch. 95).

Aristonectes parvidens

Ch. 123 (**?**) S; (**1**) O'G

Based on personal observations of MLP 40-XI-14-6

Aristonectes quiriquinensis

Ch. 123 (**?**) S; (**1**) O'G

Based on Otero et al., 2018: fig. 2, 4

Kawanectes lafquenianum

Ch. 123 (**?**) S; (**0**) O'G

Based on personal observation of the referred specimen MPEF 115

Kaiwhekea katiki

Ch. 123 (**0**) S; (**1**) O'G

Based on personal observation of OU 12649.

125. Splenial participation in mandibular symphysis: does not participate (**0**); participates (**1**). Sato (2002, Ch. 88), Druckenmiller and Russell (2008, Ch. 76), Smith and Dyke (2008, Ch. 59), Ketchum and Benson (2010, Ch. 87), Vincent et al. (2011, Ch. 37), Benson et al. (2012a, Ch. 97). Modified from O'Keefe (2001, Ch. 90), O'Keefe and Wahl (2003, Ch. 49), Albright et al. (2007, Ch. 9), O'Keefe (2008, Ch. 9), O'Keefe and Street (2009, Ch. 40) (participation of the angular in the symphysis is coded separately here by Ch. 99).

Thalassiodracon hawkinsi

Ch. 109 (**?**) S; (**1**) O'G

Based on personal observations of CAMSM J.46986, see Sfig 2A

133. Regularity of maxillary dentition: homodont (**0**); heterodont (**1**).

O'Keefe (2001, Ch. 102), Sato (2002, Ch. 105), O'Keefe and Wahl (2003, Ch. 54), Albright et al. (2007, Ch. 3), Druckenmiller and Russell (2008, Ch. 90), O'Keefe (2008, Ch. 3), O'Keefe and Street (2009, Ch. 45), Ketchum and Benson (2010, Ch. 106), Vincent et al. (2011, Ch. 44), Benson et al. (2012a, Ch. 105).

Zarafasaura oceanis

Ch. 133 (**0**) S; (**1**) O'G.

Based on Lomax and Wahl (2013:fig.5A).

138*. Number of maxillary teeth: 12–17 (**0**); 18–25 (**1**); 26–40 (**2**); >41–55 (3); >55 (4).

Modified Benson and Druckenmiller, 2014 **(different quantification)**; Benson et al.

(2012a, Ch. 108). Modified from Albright et al. (2007, Ch. 2), Druckenmiller and Russell (2008, Ch. 94), Modified from Ketchum and Benson (2010, Ch. 111), Bardet et al. (1999, Ch. 16), Sato (2002, Ch. 111), Gasparini et al. (2003, Ch. 15), Albright et al. (2007, Ch. 4), O'Keefe (2008, Ch. 4) .

Aristonectes quiriquinensis

Ch. 138(**2**) S; (**2**) O'G.

Chage of hypodigm Based on Otero et al. (2018),

Kawanectes lafquenianum

Ch. 138(**?**) S; (**0**) O'G.

Based on personal observation of MPEF 1115.

139. Cross-sectional shape of teeth in anterior half of tooth row: round or sub-rounded (**0**); sub-triangular (**1**); suboval cross-section (**2**).

Serratos et al. (2017, Ch. 139); Modified from Benson and Druckenmiller, 2014, O'Keefe (2001, Ch. 104). In the data Set of Serratos et al., (2017) several taxa were scored as "3" but no state "3" is described. It is probably the misscoring for state "2" so every "3" is change to "2".

Tuarangisaurus keyesi

Ch. 139 (**?**) S; (**2**) O'G.

Based on personal observations of the NPC CD 425 (holotype).

140. Premaxilla, diameter of first alveolus: not significantly smaller than third alveolus (**0**); less than half the diameter of third alveolus (**1**). Sato (2002, Ch. 108); modified from Benson et al. (2012b, Ch. 202), Benson et al. (2012a, Ch. 109).

Elasmosaurus platyurus

Ch. 140 (**1**) S; (**0**) O'G.

Based on personal observation of ANSP 10081 (holotype, SFig 2C).

Kaiwhekea katiki

Ch. 140 (**?**) S; (**0**) O'G.

Based on personal observations of the OU 12649 (holotype).

Tuarangisaurus keyesi

Ch. 140 (**1**) S; (**0**) O'G.

Based on personal observations of NPC CD 425 (holotype).

Libonectes morgani

Ch. 140 (**1**) S; (**0**) O'G.

Based on scoring of Serratos et al., 2017

141. Relative neck length: the neck is shorter [<0.8 times] (**0**); subequal to (**1**); or longer than [>1.2 times] trunk length (**2**). Druckenmiller and Russell (2008, Ch. 100), Vincent et al. (2011, Ch. 46).

Aristonectes quiriquinensis

Ch. 141(**1**) S; (**?**) O'G.

Based on the incompleteness of the holotype. The approximate neck length gived by Otero et al., 2014, 2018 are not a direct scoring of material and therefore it was scored as "?".

142. Axial rib articulation: articulates solely with the axis centrum (**0**); articulates partly with the atlas centrum (**1**). O'Keefe (2001, Ch. 109), O'Keefe and Wahl (2003, Ch. 58),

O'Keefe and Street (2009, Ch. 49), Ketchum and Benson (2010, Ch. 117), Benson et al. (2012a, Ch. 110).

Tuarangisaurus keyesi

Ch. 142 (**0**) S; (**?**) O'G.

Based on personal observation and O'Gorman et al. (2017). Even with the CT information it was not possible to be sure of the position of the axis rib.

145. Atlas-axis complex, hypophyseal ridge: absent or low bulge (**0**); present and prominent (**1**). Druckenmiller and Russell (2008, Ch. 97), Ketchum and Benson (2010, Ch. 115), Benson et al. (2012a, Ch. 112).

Aristonectes parvidens

Ch. 145 (**1**) S; (**0**) O'G.

Based on personal observation and see O'Gorman (2016a:fig. 9.1, 2).

Tuarangisaurus keyesi

Ch. 145 (**1**) S; (**0**) O'G.

Based on personal observation O'Gorman et al. (2017:fig. 9:5, 6).

147. Atlas-axis complex, hypophyseal ridge location: extends across both atlantal centrum, and axial centrum (**0**); does not contact the axial centrum (**1**); inapplicable, hypophyseal ridge absent (**?**). Benson and Druckenmiller (2014).

Tuarangisaurus keyesi

Ch. 147 (**1**) S; (**?**) O'G.

Following the change in the scoring of Ch. 145.

152. Number of cervical vertebrae: <15 (**0**); 18–23 (**1**); 24–29 (**2**); 30–36 (3); 37–49 (4); 50–59 (5); >60 (6).

Modified from Bardet et al. (1999, Ch. 19), Carpenter (1999, Ch.s 12–15), O'Keefe (2001, Ch. 2), Sato (2002, Ch.s 117–118), Gasparini et al. (2003, Ch. 17), O'Keefe and Wahl (2003, Ch.s 2, 60), Albright et al. (2007, Ch. 13), Großmann (2007, Ch. 27), Druckenmiller and Russell (2008, Ch. 99), O'Keefe (2008, Ch. 13), O'Keefe and Street (2009, Ch. 51), Ketchum and Benson (2010, Ch. 118), Modified from Benson et al. (2012a, Ch. 115).

Aristonectes quiriquinensis

Ch. 152 (4) S; (**?**) O'G.

Based on the absence of complete cervical region of *A. quiriquinensis*

153. Proportions of anterior–middle cervical centra: substantially shorter than high [length <0.7 x height] (**0**); approximately as long as high 0.7-1.1 (**1**); substantially longer than high 1.1-1.5 (**2**). Even longer can shaped (Otero et al., 2016; O'Keefe and Hiller, 2006 (**3**).

Futabasaurus suzuki

Ch. 153 (**1**) S; (**2**) O'G.

Based on the available vertebrae proportions and the observed tendency.

154. Lateral surfaces of anterior cervical centra (**excluding posteriormost cervicals**)**:** longitudinal ridge absent (**0**); present (**1**). Bardet et al. (1999, Ch. 22), Carpenter (1999, Ch. 17), O'Keefe (2001, Ch. 115), Gasparini et al. (2003, Ch. 19), Großmann (2007, Ch. 30),

Druckenmiller and Russell (2008, Ch. 103), Ketchum and Benson (2010, Ch. 121), Benson et al. (2012a, Ch. 118). Modified from Sato (2002, Ch.s 123–124), Sato (2002, Ch. 122).

Gronausaurus wegneri

Ch. 154 (**?**) S; (**?**) O'G.

Aristonectes parvidens

Ch. 154 (**1**) S; (**0**) O'G.

Based on personal observations. See discussion in O'Gorman (2016).

Zarafasaura oceanis

Ch. 154 (**1**) S; (**0**) O'G.

Based on Lomax and Wahl (2013) and photographic material provided by D. Lomax and B. Wahl (Wyoming Dinosaur Center).

155*. Cervical centra, ventral notch: absent, centra subcylindrical (**0**); present, centra 'dumbell' or 'binocular' shaped in anterior to median cervical centra (**1**). Ventral notch present in posterior cervical centra (**15th pre-pectoral centra) (2).** Bardet *et al.* (1999, Ch. 23), modified from O'Keefe (2001, Ch. 116), Sato (2002, Ch. 121), Gasparini *et al.* (2003, Ch. 20), Druckenmiller and Russell (2008*a*, Ch. 104), O'Keefe and Street (2009, Ch. 55), Ketchum and Benson (2010, Ch. 122), Vincent *et al.* (2011, Ch. 49).

157. Anterior cervical neural spines, morphology: curve posterodorsally (**0**); inclined straight posterodorsally (**1**); inflected dorsally to anterodorsally (**2**); inapplicable in some pistosaurians that have extremely low neural spines (**?**). Benson et al. (2012a, Ch. 119). Modified from Sato (2002, Ch. 135), Modified from O'Keefe (2001, Ch. 125), O'Keefe

and Wahl (2003, Ch. 70), Druckenmiller and Russell (2008, Ch. 111), Smith and Dyke (2008, Ch. 70), O'Keefe and Street (2009, Ch. 61), Vincent et al. (2011, Ch. 50). Modified from Otero et al. (2012:61).

Albertonectes vanderveldei

Ch. 157 (**2**) S; (**1**) O'G

Based on personal observation of TMP 2007.011.0001 (fig. S3E).

Aristonectes parvidens

Ch. 157 (**?**) S; (**0**) O'G.

Based on personal observation of the MLP 40-XI-14-6

Aristonectes quiriquinensis

Ch. 157 (**2**) S; (**?**) O'G.

Based on personal observation of the hypodigm SGO.PV.957

Elasmosaurus platyurus

Ch. 157(**?**) S; (**0**) O'G

Based on personal observations of ANSP 10081 (SFig 3C).

Kaiwhekea katiki

Ch. 157 (**1**) S; (**2**) O'G.

Based on personal observation the anteriormost cervical are not well preserved and therefore the ? is preferred.

Kawanectes lafquenianum

Ch. 157 (**2**) S; (**?**) O'G.

Based on personal observation of the hypodigm. No well preserved neural spine of anterior cervical vertebrae is present.

Nakonanectes bradti

Ch. 157 (0) S; (**2**) O'G

Based on state modification and Serratos et al. (2017:fig.8B, E).

Tuarangisaurus keyesi

Ch. 157 (**1**) S; (**0**) O'G

Based on personal observation see O'Gorman et al. (2017:fig 10C).

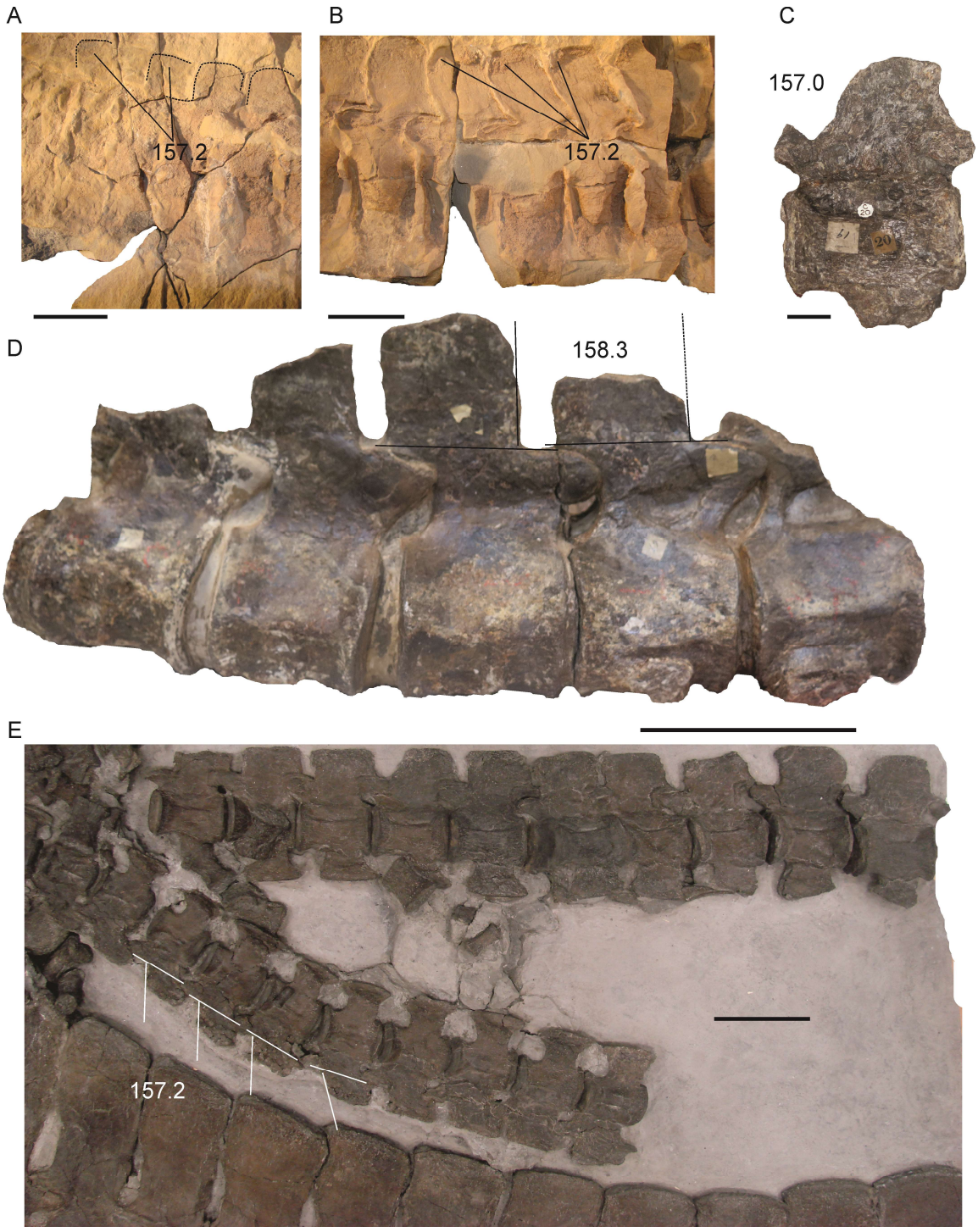

FIGURE S3**. A**, **B**, *Kaiwhwkea katiki* (OU 12649) anterior cervical centra (natural casts). Scale bar equals 20 mm. **C**-**D**, *Elasmoasurus platyurus* (ANSP 10081, holotype), **C**, anterior cervical vertebrae in left lateral view. Scale bar equals 20 mm. **D**, posterior cervical

vertebrae in right lateral view. Scale bar equals 20 mm. **E**, *Albertonectes vanderveldei* (TMP 2007.011.0001, holotype) anterior cervical vertebrae in right view. Scale bar equals 100 mm.

158*. Posterior cervical neural spines, morphology: curve posterodorsally (**0**); inclined straight posterodorsally (**1**); strongly inflected anterodorsally (**2**); **no anterior or posterior inflexion** (**3**); inapplicable in some pistosaurians that have extremely low neural spines (**?**). Modified from Benson and Druckenmiller, 2014, Benson et al. (2012a, Ch. 120). Modified from Sato (2002, Ch. 136). Modified from O'Keefe (2001, Ch. 125), O'Keefe and Wahl (2003, Ch. 70), Druckenmiller and Russell (2008, Ch. 111), Smith and Dyke (2008, Ch. 70), O'Keefe and Street (2009, Ch. 61), Vincent et al. (2011, Ch. 50); Modified from Otero et al. (2012: Ch. 61).

Albertonectes vanderveldei

Ch. 158 (**2**) S; (3) O'G

Based on personal observation of TMP 2007.011.0001 (holotype, Fig. S4C)

Brancasaurus brancai

Ch. 158 (**0**) S; (**1**) O'G

Based on Sach and Kear (2016: 16A) and Hampe (2013:fig 5A).

Callawayasaurus colombiensis

Ch. 158 (**2**) S; (**1**) O'G

Based on personal observation of UCPM 38349 (holotype, Fig. S4A).

Elasmosaurus platyurus

Ch. 158 (**2**) S; (3) O'G

Based on personal observation of ANSP 10081 (Fig. S3D).

Hydrotherosaurus alexandrae

Ch. 158 (**2**) S; (3) O'G

Based on personal observation of UCMP 33912 (holotype, Fig. S4B).

***Styxosaurus* sp**.

Ch. 158 (**2**) S; (3) O'G

Based on personal observation of AMNH 1495+AMNH 5835 and new state (3).

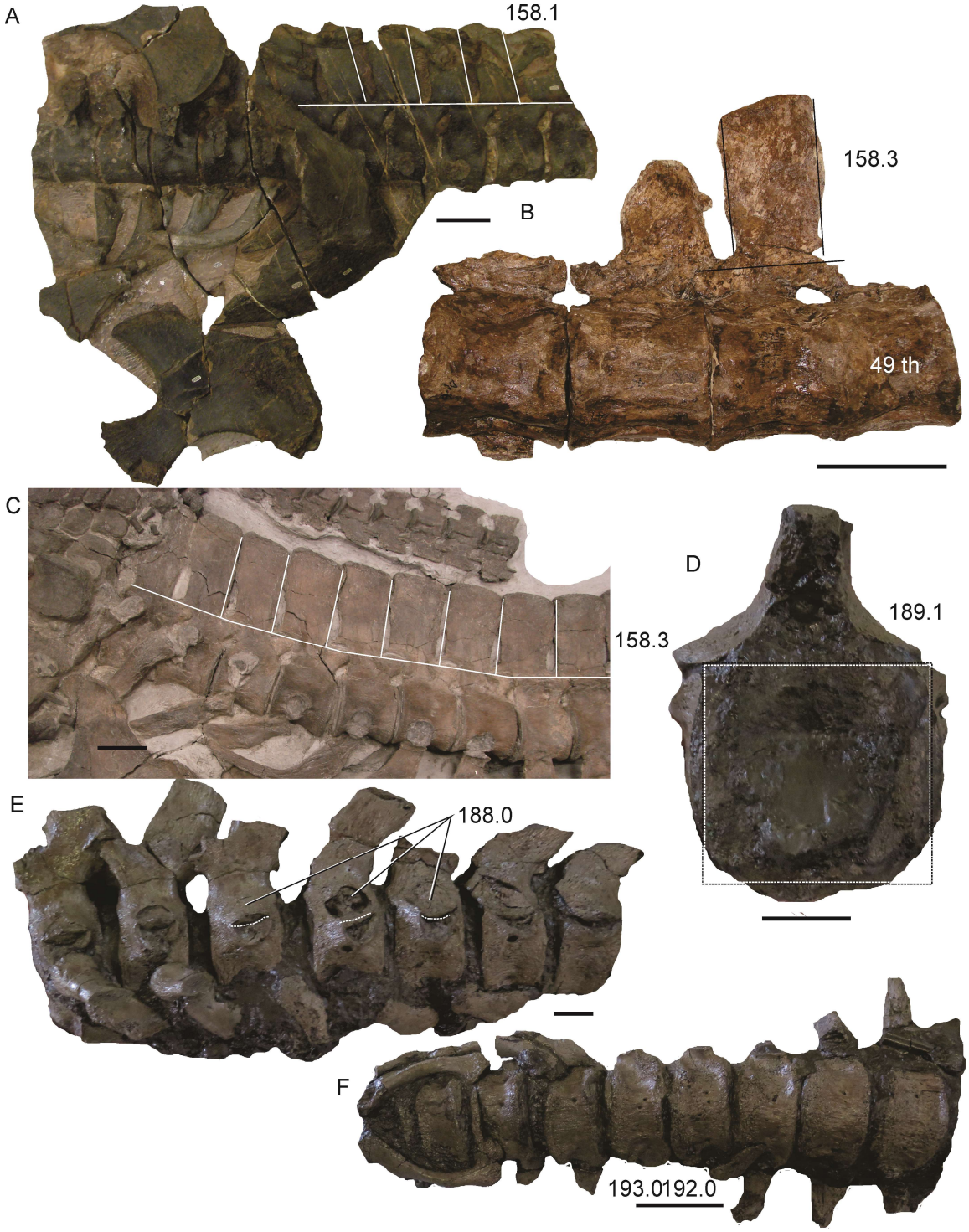

FIGURE S4**. A**, *Callawayasaurus colombiensis* (UCPM 38349 holotype) posterior cervical, anerior dorsal vertebrae in left lateral view, clavicle-interclavicle complex and scapula. Scale barequals 100 mm. **B**, *Hydrotherosaurus alexandrae* (UCMP 33912, holotype) posterior cervical in left lateral view. Scale equals 100 mm. **C**, *Albertonectes vanderveldei* (TMP 2007.011.0001, holotype) posterior cervical centra in right lateral view.

Scale bar equals 100 mm. **D-F**, *Hauffiosaurus tomistomimus* (MANCH LL 8004, holotype), **D**, middle caudal vertebrae in posterior view. Scale bar equals 20 mm. **E**, middle caudal vertebrae in left lateral view. Scale bar equals 20 mm, **F**, middle caudal vertebrae in ventral view. Scale bar equals 50 mm.

159. Posterior cervical neural spines, height relative to centrum: substantially shorter than centrum (**0**); subequal (**1**); substantially taller [equal to or greater than 1.2 times centrum height] (**2**). Benson et al. (2012aa, Ch. 121). Modified from Ketchum and Benson (2010, Ch. 130) (Ch. restricted to posterior cervical neural spines; anterior neural spines coded by Ch. 171).

Elasmosaurus platyurus

Ch. 159 (**2**) S; (**?**) O'G

Based on personal observation (ANSP 10081), the posterior neural spines are too damages to know its original length.

Futabasaurus suzukii

Ch. 159 (**2**) S; (**1**) O'G

Based on Sato et al. (2006:fig. 5A-C).

Kaiwhekea katiki

Ch. 159 (**2**) S; (**1**) O'G

Based on personal observation of OU 12649.

165. Cervical centra, median ventral surface: approximately flat or convex (**0**); bears a rounded midline ridge [*cf*. Tarlo, 1960] (**1**); or bears a sharp keel (**2**).

Druckenmiller and Russell (2008, Ch. 105), Benson et al. (2012a, Ch. 126). State 2 from O'Keefe (2001, Ch. 114), O'Keefe and Wahl (2003, Ch. 63), Smith and Dyke (2008, Ch.s 64, 67), O'Keefe and Street (2009, Ch. 54). Modified from Sato (2002, Ch.s 125–126)

(separate Ch.s for anterior and posterior cervical vertebrae lumped together here). Modified from Ketchum and Benson (2010, Ch. 123).

This is a character difficult to score because all elasmosaurids shows some kind of ventral keel between ventral foramina on cervical centra, additionally the ventral keel development is variable along the cervical region. Therefore all elasmosaurids that where reviewed personally where scored as (**1**), rounded keel. This probably did not represent accurately the variation but probably it is the better option of scoring avoiding extremely subjective scorings.

168. Cervical zygapophyses, median contact between left and right zygapophyseal facets: absent for most/all of length (**0**); present for most of anteroposterior length (**1**).-Sato (2002, Ch. 132), Druckenmiller and Russell (2008, Ch. 109), Ketchum and Benson (2010, Ch. 128) Modified from Benson et al. (2012b, Ch. 128), Benson et al. (2012a, Ch. 129) .

Brancasaurus brancai

Ch. 168 (**0**) S; (0/1) O'G

Sach and Kear, 2016 (fig 15B) shows that anteriormost cervicals prezigapophyses did not contact each other on the midline. However the postzigapofisis are progressively confluent.

172. Cervical vertebrae, shape of neurocentral suture in anterior–middle cervical vertebrae in lateral view: rounded, ventrally convex (**0**); V-shaped (**1**); extends far ventrally so that neural arch contacts dorsal part of rib facet (**2**); extends far ventrally but is evenly convex and does not contact rib facet (**3**).

Benson et al. (2012a, Ch. 132). State 2 from Ketchum and Benson (2010, Ch. 126).

Kaiwhekea katiki

Ch. 172 (**0**) S; (**?**) O'G

Based on personal observations, it was impossible to determine the state of this character.

173*. Cervical centrum, proportional width: mediolateral width subequal to height or less (**0**); at least 1.2 times as wide mediolaterally as high dorsoventrally (**1**). **Extremely anterior cervical vertebrae width at least 1.3 and ratio B/L more than 1.30 in anterior half of neck or extremely high B/L in posterior cervical** (**2**). **Modified** from Benson et al. (2012a, Ch. 133) by addition of state 3

Aristonectes parvidens

Ch. 173 (**0**) S; (**2**) O'G

Based on personal observation and O'Gorman (2016a).

Aristonectes quiriquinensis

Ch. 173 (**0**) S; (**2**) O'G

Based on personal observation and Otero et al. (2014).

Kaiwhekea katiki

Ch. 173 (**0**) S; (**2**) O'G

Based on personal observation and Cruickshank and Fordyce (2002).

179*. Number of dorsal vertebrae: 17–19 (**0**); >20 (**1**);

Modified by different quantification. Sato (2002, Ch. 119), Ketchum and Benson (2010, Ch. 135), Benson et al. (2012a, Ch. 138) (different quantifications).

Aristonectes quiriquinensis

Ch. 179 (**?**) S; (**1**) O'G

Based on Otero et al., 2014, 2018 and Otero com. pers. (new preparation indicate 24 dorsal vertebrae)

Brancasaurus brancai

Ch. 179 (**1**) S; (**0**) O'G

Based on modification of character 179.

Callawayasaurus colombiensis

Ch. 179 (**2**) S; (**?**) O'G

Based on personal observation of the postcranium of both specimens (holotype, UCPM 38349 and "Bogota specimen" of Welles (1962) RA4425, postcranium none preserved a complete (UCPM 38349) or easy to determine (RA4425) the number of dorsal vertebrae.

Vegasaurus molyi

Ch. 179 (**1**) S; (**0**) O'G

Based on O'Gorman et al. (2015) who determine 17 dorsal vertebrae

180. Number of pectoral vertebrae: 2–4 (**0**); 5–7 (**1**). Benson et al. (2012a, Ch. 139). 'Pectoral' vertebrae are those in which the rib facet comprises portions of both the centrum and neural arch (Seeley, 1874).

Elasmosaurus platyurus

Ch. 180 (?) S; (**0**) O'G

Based on pers. obs. 2017 (ANSP 10081) and Sachs et al. (2013:fig. 3A).

184. Dorsal neural spines, mediolateral width of apices in mid–posterior dorsal neural spines: unexpanded, transversely narrow relative to anteroposterior width (**0**); mediolaterally thick, subequal to anteroposterior width (**1**); alternate spines expanded

laterally to one side (**2**). Benson et al. (2012a, Ch. 144). Modified from Benson et al. (2012b, Ch. 211).

Gronausaurus wegneri

Ch. 184 (**0**) S; (**2**) O'G

Based on Hampe (2013:fig 5F).

188. Caudal ribs facet location in proximal–middle caudal vertebrae: located dorsally, contacting or almost contacting neural arch (**0**); placed dorsally but neural arch does not form part of facet (**1**); at midheight of centrum or lower (**2**). Benson et al. (2012a, Ch. 149).

Brancasaurus brancai/Gronausaurus wegneri

Both specimen where scored as 0/1 based on the presence of polymorphism in this character, at least in the anteriormost caudals (see Hampe, 2013:fig. 6A; Sach and Kear: 2016: 17B).

Hauffiosaurus tomistomimus

Ch. 188 (**?**) S; (**0**) O'G

Based on personal observations of MANCH LL 8004 (Fig. S4E)

Terminonatator ponteixensis

Ch. 188 (**1**) S; (**?**) O'G

Based on Sato, 2003 it is not clear the scoring of this characters and therefore ? is selected.

189*. Caudal centra, outline of middle caudal centra in anterior view: suboval (**0**); subrectangular, chevron facets widely spaced and located ventrolaterally, ventral surface approximately flat giving a subrectangular appearance to centrum in anterior view (**1**).

Large parapophysis located at the level of the lateral surface giving an octagonal shaped outline (2) Benson et al. (2012a, Ch. 150). Modified from Otero, 2016 Ch. 189.

Aristonectes parvidens

Ch. 189 (**0**) S; (**2**) O'G

Based on personal observations of MLP 40-XI-14-6.

Aristonectes quiriquinensis

Ch. 189 (**?**) S; (**2**) O'G

Based on Otero et al., 2018.

Callawayasaurus colombiensis

Ch. 189 (**?**) S; (**0**) O'G

Based on personal observation of the Bogota specimen: UCPM 125328 (skull) and RA4425 (postcranium).

Hauffiosaurus tomistomimus

Ch. 189 (**?**) S; (**1**) O'G

Based on personal observation of MANCH LL 8004 (Fig. S4D).

190. Caudal centra, length: height ratio of proximal caudal centra: >0.85 (**0**); 0.6-0.8 (**1**); <0.55 (**2**). Benson et al. (2012a, Ch. 151).

Aristonectes parvidens

Ch. 190 (**?**) S; (**1**) O'G

Based on personal observations of MLP 40-XI-14-6 and O'Gorman, 2016a.

Zarafasaura oceanis

Ch. 190 (**?**) S; (**1**) O'G

Based on and photographic material of WDC CMC-01 provided by D. Lomax and B. Wahl (Wyoming Dinosaur Center).

191. Caudal centrum, subcentral foramina on ventral surface: paired lateral foramina (**0**); single midline foramen (**1**); **more than two foramen in several caudal vertebrae (2).** Benson and Druckenmiller (2014).

Albertonectes vanderveldei

Ch. 191 (**?**) S; (1) O'G

Based on personal observations of TMP 2007.011.0001.

Aristonectes parvidens

Ch. 191 (**?**) S; (**2**) O'G

Based on personal observation of MLP 40-XI-14-6 see O'Gorman, 2016a:fig.11.3

Aristonectes quiriquinensis

Ch. 191 (**?**) S; (**2**) O'G

Based on personal observation, see Otero et al. (2018:fig. 11F).

Zarafasaura oceanis

Ch. 191 (**?**) S; (**2**) O'G

Based on and photographic material of WDC CMC-01 provided by D. Lomax and B. Wahl (Wyoming Dinosaur Center).

Naconanectes bradti

Ch. 191 (**1**) S; (0/1) O'G

Based on Serratos et al. (2017).

192. Caudal vertebrae, chevron facet: located equally on anterior and posterior edges of the centrum (**0**) or mainly on the posterior edge, low, mound-like eminence may be present on ventrolateral surface of centrum anteriorly (**1**). Modified from Albright et al. (2007, Ch. 16), O'Keefe (2008, Ch. 16).

Hauffiosaurus tomistomimus

Ch. 192 (**?**) S; (**0**) O'G

Based on personal observation of MANCH LL 8004

193. Middle and distal caudal vertebrae, chevron facets: flush with level of ventral surface of centrum (**0**); project significantly ventrally (**1**). Benson et al. (2012a, Ch. 152).

Albertonectes vanderveldei

Ch. 193 (**1**) S; (0/1) O'G

Based on personal observations of TMP 2007.011.0001 (holotype).

Hauffiosaurus tomistomimus

Ch. 193 (**?**) S; (**0**) O'G

Based on personal observation of MANCH LL 8004 (Fig. S 4F).

Aristonectes parvidens

Ch. 193 (**?**) S; (**0**) O'G

Based on personal observation, see O'Gorman, 2016a:fig.11.3, 4

Kawanectes lafquenianum

Ch. 193 (**1**) S; (0/1) O'G

Based on personal observation of MLP 71-II-13-1 (holotype); MCS PV 4; MUC Pv 92.

Kaiwhekea katiki

Ch. 193 (**0**) S; (**?**) O'G

Based on personal observation of OU 12649, I was not capable of observe ventral surfaces of caudal vertebrae.

Vegasaurus molyi

Ch. 193 (**1**) S; (**0**) O'G

Based on personal observation of MLP 93-I-5-1 (holotype).

Terminonatator ponteixensis

Ch. 193 (**?**) S; (**1**) O'G

Based on Sato et al. (2003:fig. 10D).

196. Ratio of coracoid to scapular length: > or equal to 1.9 (0); 1.6–1.9 (1) < or equal to 1.6 (2). Modified from O'Keefe (2001, Ch. 4), Sato (2002, Ch. 160), Druckenmiller and Russell (2008*a*, Ch. 125), Smith and Dyke (2008, Ch. 76), Ketchum and Benson (2010, Ch. 147), Benson *et al.* (2012*a*, Ch. 154).

Callawayasaurus colombiensis

Ch. 196 (**?**) S; (**2**) O'G.

Based on Welles (1952):fig. 2.

197. Anteromedial margin of the coracoid: does not contact the scapula (**0**); contacts the scapula (**1**). Sato (2002, Ch. 169), Smith and Dyke (2008, Ch. 79), O'Keefe and Street (2009, Ch. 89), Ketchum and Benson (2010, Ch. 144), Benson et al. (2012a, Ch. 155). Modified from O'Keefe (2001, Ch. 137), O'Keefe and Wahl (2003, Ch. 77), Druckenmiller and Russell (2008, Ch. 122), O'Keefe and Street (2009, Ch. 68), Modified from Sato (2002, Ch. 158).

Zarafasaura oceanis

Ch. 197 (**?**) S; (**1**) O'G.

Based on Lomax and Wahl, (2013:fig. 10).

200. Contact of the ventral plates of the scapulae along the midline: do not meet along the midline (0); meet along the ventral midline (1). Bardet et al. (1999, Ch. 24), Carpenter (1999, Ch. 19), Sato (2002, Ch. 156), Druckenmiller and Russell (2008, Ch. 123), Smith and Dyke (2008, Ch. 80), O'Keefe and Street (2009, Ch. 66), Ketchum and Benson (2010, Ch. 145), Vincent et al. (2011, Ch. 56), Benson et al. (2012a, Ch. 158). Modified from O'Keefe (2001, Ch. 135), O'Keefe and Wahl (2003, Ch. 75).

Callawayasaurus colombiensis

Ch. 200 (**0**) S; (0/1) O'G.

The scoring of this character is "0" follows the figures of Welles, 1962:fig 5 and Druckenmiller and Russell, 2006: 10B. However Welles (1962:fig. 6b) indicates the presence of scapular symphysis on the Bogota specimen (Fig. S5D). Personal observation of the Bogota specimen indicates the same.

Zarafasaura oceanis

Ch. 197 (**?**) S; (**1**) O'G.

Based on Lomax and Wahl (2013:fig. 10).

202. Shape of the anterolateral margin of the scapula where the dorsal ramus (dorsolateral process) meets the ventral ramus: flat or gently convex (**0**); forms prominent ridge or shelf (**1**); inapplicable, ventral plate not developed (**?**). Sato (2002, Ch.

157), Druckenmiller and Russell (2008, Ch. 124), Ketchum and Benson (2010, Ch. 146), Benson et al. (2012a, Ch. 160).

Hauffiosaurus tomistomimus

Ch. 202 (**?**) S; (**1**) O'G.

Based on personal observation of MANCH LL 8004 (holotype, Sfig 5A).

203. Scapular blade (dorsolateral process), anteroposterior width at distal end: subequal to width at midlength (**0**); narrow, tapering dorsally (**1**); broad, distal part expanded relative to midlength (**2**). Benson et al. (2012a, Ch. 161). Modified from O'Keefe (2001, Ch. 132), Sato (2002, Ch. 159), Ketchum and Benson (2011*a*, Ch. 196).

Aristonectes quiriquinensis

Ch. 203 (**1**) S; (**0**) O'G.

Based on Otero et al. (2014 fig. 13A, B).

Kaiwhekea katiki

Ch. 203 (**?**) S; (**0**) O'G.

Based on personal observation of OU 12649 (Fig. S5D).

Vegasaurus molyi

Ch. 203 (**1**) S; (**0**) O'G.

Based on personal observation of MLP 93-I-5-1 (holotype) and O'Gorman et al. (2015:fig. 8).

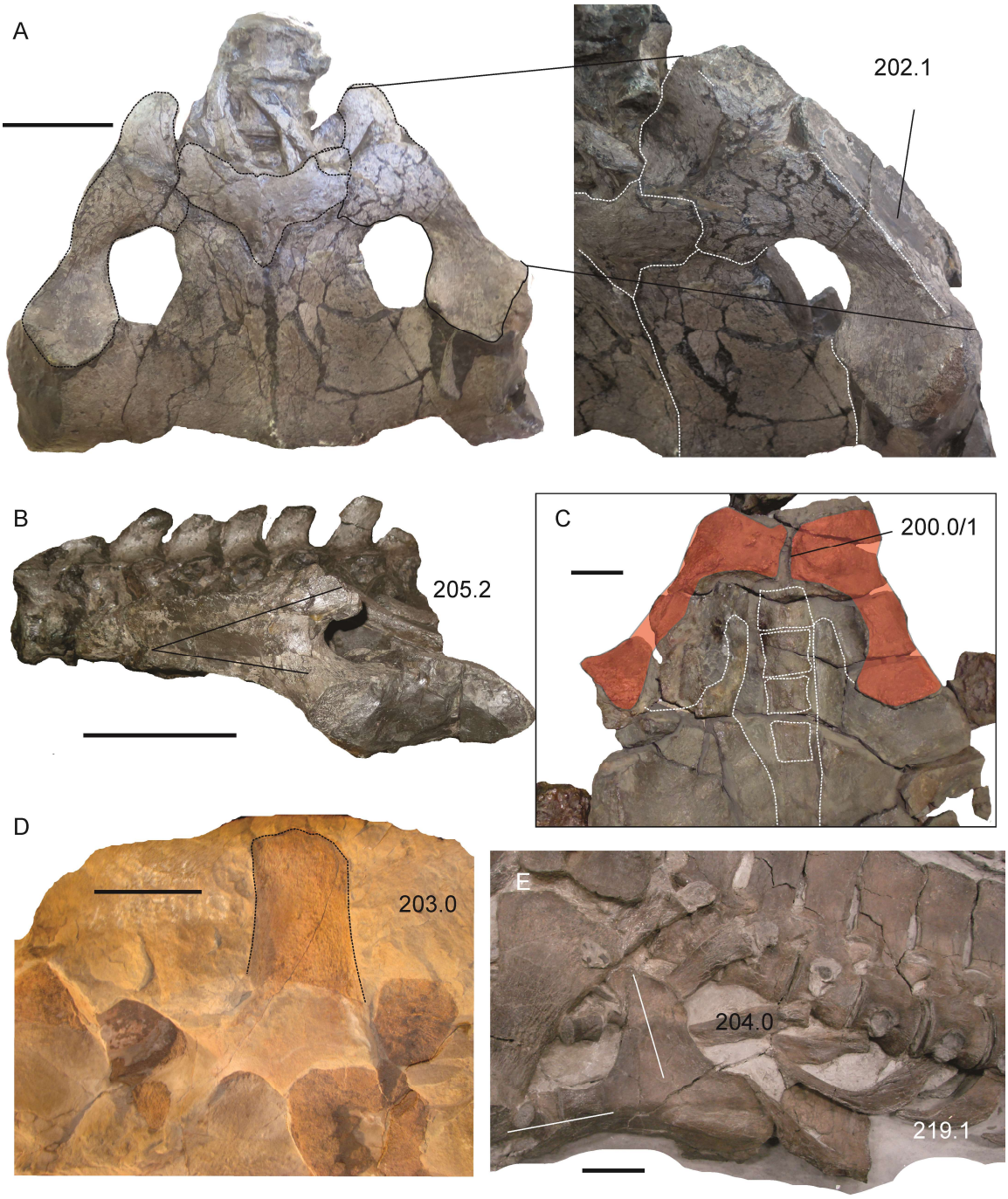

FIGURE S5. Scapula characters modifications. **A**, **B**, *Hauffiosaurus tomistomimus* (MANCH LL 8004, holotype), A, pectoral girdle in ventral and latero-ventral view. Scale

bar equals 100 and B, scapula in left lateral view. Scale bar equals 100 mm. **C**, *Callawayasaurus colombiensis* (RA4425, Bogota specimen). Scale bar equals 100 mm. **D**, *Kaiwhekea katiki* (OU 12649, holotype) Scale bar equals 100 mm. **E**, *Albertonectes vanderveldei* (TMP 2007.011.0001, holotype), left scapula in lateral view. Scale bar equals 100 mm.

204. Scapula blade, length relative to posterior process of scapula: blade longer between 1.2 and 1.5 (**0**); blade subequal to or shorter than (**1**); blade longer than 1.5 posterior process length (**2**). Modified from Benson and Druckenmiller (2014 Ch. 204) by addition of state 2.

Albertonectes vanderveldei

Ch. 204 (**1**) S; (**0**) O'G.

Based on personal observation of TMP 2007.011.0001(holotype, Fig. S5E).

Aristonectes quiriquinensis

Ch. 204 (**1**) S; (**0**) O'G.

Based on Otero et al. (2014:fig. 13A, B).

Elasmosaurus platyurus

Ch. 204 (**1**) S; (**?**) O'G.

As the scapula ANSP 10081 is no available this character could be cheeked with certainty

Kawanectes lafquenianum

Ch. 204 (**?**) S; (**2**) O'G.

Based on personal observation of MCS 4.

Vegasaurus molyi

Ch. 204 (**1**) S; (**2**) O'G.

Based on personal observation and O'Gorman et al. (2015:fig.8D-G).

205. Scapula blade, angle relative to ventral scapula margin: vertical/subvertical [70–90 degrees] (**0**); intermediate posterodorsal inclination [45–60 degrees] (**1**); strong posterodorsal inclination [30–45 degrees] (**2**). Benson and Druckenmiller, 2014.

Hauffiosaurus tomistomimus

Ch. 205 (**?**) S; (**2**) O'G.

Based on personal observation of MANCH LL 8004. (Sfig 5B).

Elasmosaurus platyurus

Ch. 205 (**0**) S; (**?**) O'G.

As the scapula ANSP 10081 is no available this character could be cheeked with certainty

207. Coracoid, posterolateral cornu: does not extend as far laterally as glenoid (**0**); extends to level of glenoid (**1**); extends lateral to glenoid (**2**). Ketchum and Benson (2011*a*, Ch. 151), Benson et al. (2012a, Ch. 163). Modified from Bardet et al. (1999, Ch. 25), O'Keefe (2001, Ch. 142), Sato (2002, Ch. 166), Großmann (2007, Ch. 32), Druckenmiller and Russell (2008, Ch. 128), Ketchum and Benson (2010, Ch. 151), Modified from Vincent et al. (2011, Ch. 57) , Smith and Dyke (2008, Ch. 75).

Vegasaurus molyi

Ch. 205 (**2**) S; (**?**) O'G.

Based on personal observation of MLP 93-III-3-1, Figures 8A, 9A, B of O'Gorman et al. (2015) is quite tricky because the posterior part of the coracoids is broken and affected by a fault so the general shape is not completely natural.

208. Coracoid, median fenestra/large embayment: absent, although intercoracoid contact may be slightly split posteriorly (**0**); median embayment present and posteriorly opened (**1**); posterior processes strongly divergent forming prominent V-shaped or otherwise mediolaterally narrow emargination (**2**). Present but closed (**3**).

"Speeton Clay Plesiosaurian"

Ch. 208 (**?**) S; (**1/3**) O'G.

215. Coracoid, ventral projection/process extends from intercoracoid symphysis: absent (**0**); present (**1**). Sato (2002, Ch. 167: 'knob on the median symphysis of coracoids').

Hydrotherosaurus alexandrae

Ch. 215 (**0**) S; (**?**) O'G.

Based on personal observation of UCMP 33912. As could be observed the area is too damage to determine if the ventral process was or not present (Fig. S6A).

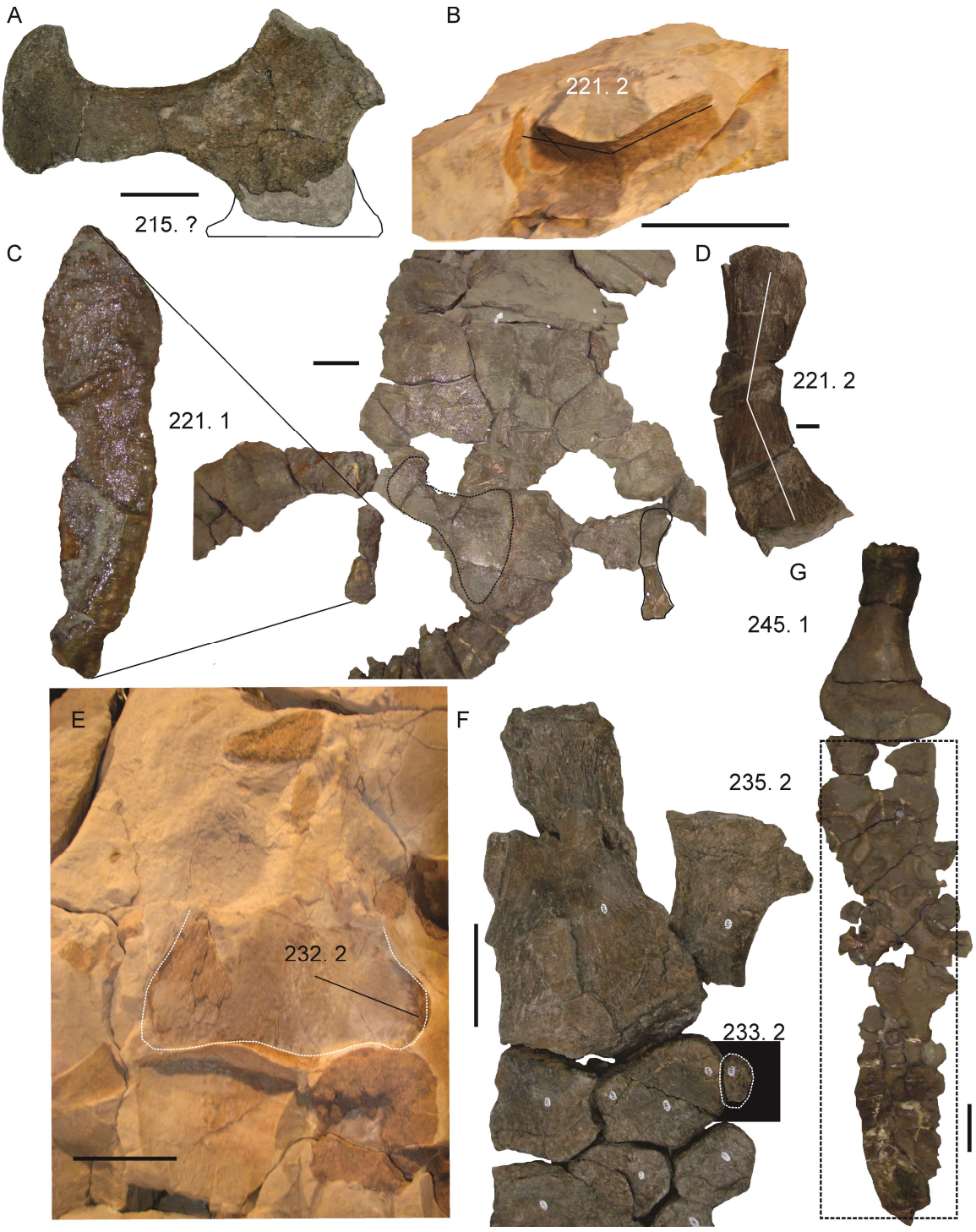

FIGURE S6**. A**, *Hydrotherosaurus alexandrae* (UCMP 33912, holotype), coracoid in ventral view. Scale bar equals 100. **B**, *Kaiwhekea katiki* (OU 12649, holotype). **C**, *Callawayasaurus colombiensis* (RA4425, Bogotá Specimen), right ilium in lateral view.

Scale bar equals 100 mm. **D**, *Albertonectes vanderveldei* (TMP 2007.011.0001, holotype), right ilium in lateral view. Scale bar equals 20 mm. **E**, *Kaiwhekea katiki* (OU 12649, holotype), humerus (cast). Scale bar equals 100 mm. **F**, *Hydrotherosaurus alexandrae* (UCMP 33912, holotype); left anterior limb in dorsal view. Scale bar equals 100 mm. **G**, *Callawayasaurus colombiensis* (RA4425, Bogotá specimen). Scale bar equals 100 mm.

219. Clavicle/interclavicle complex, shape of anterior margin: markedly concave, mediolateral width of concavity at least 1.25 times the anteroposterior depth (**0**); anteriorly convex or pointed (**1**); transversely broad and almost straight (**2**); small, transversely narrow, weakly concave region (**3**).

Libonectes morgani

Ch. 219 (**?**) S; (**0**) O'G.

Based on Welles 1952:fig. 2

218. Contact of the clavicles along the midline: present (**0**); absent (**1**).

Druckenmiller and Russell (2008, Ch. 120), Ketchum and Benson (2010, Ch. 142).

Modified from O'Keefe (2001, Ch. 134), Sato (2002, Ch. 152), O'Keefe and Wahl (2003, Ch. 74).

Callawayasaurus colombiensis

Ch. 218 (**0**) S; (**?**) O'G.

Based on personal observations, no suture is visible on the UCPM 38349

or RA4425 (Bogota specimen of Welles, 1962).

Futabasaurus suzukii

Ch. 218 (**1**) S; (**?**) O'G.

Based on Sato et al., 2006, no suture are visible. And therefore the score ? was considered.

219. Clavicle/interclavicle complex, shape of anterior margin: markedly concave, mediolateral width of concavity at least 1.25 times the anteroposterior depth (**0**); anteriorly convex or pointed (**1**); transversely broad and almost straight (**2**); small, transversely narrow, weakly concave region (3). Modified from Benson et al. (2012b, Ch. 141); Benson et al. (2012a, Ch. 170).

Albertonectes vanderveldei

Ch. 219 (**?**) S; (**1**) O'G.

Based on personal observation of the TMP 2007.011.0001 (holotype, SFig 5E).

.

221. Ilium curvature shaft in lateral view: appears straight, pelvic articular end equally expanded anteriorly and posteriorly (**0**); curves anterodorsally, articular end expanded only anteriorly less arched than state 2 (**1**); sigmoidal equally two sections and strongly arched (**2**). Modified from Sato (2002, Ch. 170), Benson and Druckenmiller (2014: Ch. 221), Albright et al. (2007, Ch. 29), O'Keefe (2008, Ch. 29), Druckenmiller and Russell (2008, Ch. 142), Ketchum and Benson (2010, Ch. 167), Vincent et al. (2011, Ch. 60), Benson et al. (2012a, Ch. 172).

Callawayasaurus colombiensis

Ch. 221 (**?**) S; (**1**) O'G.

Base on direct observation of RA4425 (Bogota Specimen of Welles, 1962, Fig. S6C).

Zarafasaura oceanis

Ch. 221 (**1**) S; (**0**) O'G.

Lomax and Wahl, 2013:fig. 12 and photographic material of WDC CMC-01 provided by D. Lomax and B. Wahl (Wyoming Dinosaur Center).

Albertonectes vanderveldei

Ch. 221 (**1**) S; (**2**) O'G.

Based on personal observation of TMP 2007.011.0001 (holotype, SFig 6D).

Kaiwhekea katiki

Ch. 221 (**?**) S; (**2**) O'G.

Based on personal observation of OU 12649 (holotype, Fig. S6B).

Kawanectes lafquenianum

Ch. 221 (**1**) S; (**2**) O'G.

Based on personal observation on the holotype MLP 71-II-13-1 and O'Gorman (2016 fig. 6.3, 4).

Vegasaurus molyi

Based on personal observation on the holotype MLP 93-I-5-1 and O'Gorman et al, 2015 fig. 10C, D.

"Speeton Clay Plesiosaurian" (SCARB200751)

Ch. 221(**2**) S; (**1**) O'G

Based on personal observation of SCARB200751 (on display).

224. Ilium, anteroposterior width of dorsal expansion: tapering, less than minimum shaft width (**0**); slight, just greater than minimum shaft width (**1**); expanded, between 1.5–2.0 times the minimum anteroposterior widths of the shaft (**2**); large, over 2.5 times minimum shaft width (3). Benson et al. (2012a, Ch. 175). Modified from Ketchum and Benson (2011*a*, Ch. 201), Sato (2002, Ch. 172).

Elasmosaurus platyurus

Ch. 224 (**2**) S; (**?**) O'G.

As the ilium is no available this character could be cheeked with certainty and therefore the scored "?" is preferred.

225. Ilium, tubercle on posterior surface around midlength: absent (0); present as a tubercle (1); rugose, proximodistally oriented crest present (2).

Benson *et al.* (2012*a*, Ch. 176). Modified from Ketchum & Benson (2011*a*, Ch. 198) (addition of state 2).

Elasmosaurus platyurus

Ch. 225 (**0**) S; (**?**) O'G.

Based on the fact of the non preservation of the material.

227. Ilium ratio of length to minimum anteroposterior width: <3.0 (**0**); 4.0–5.2 (**1**); >5.3 (**2**).

Benson et al. (2012a, Ch. 177).

Modified from Smith and Dyke (2008, Ch. 85).

Zarafasaura oceanis

Ch. 227(**2**) S; (**1**) O'G.

Based on Lomax and Wahl, 2013 and photographic material of WDC CMC-01 provided by D. Lomax and B. Wahl (Wyoming Dinosaur Center).

230. Pubis, anterolateral cornu: absent or weak and rounded, extending less far laterally than acetabulum (**0**); or present, extending further laterally than acetabulum (**1**). Sato (2002, Ch. 174), Druckenmiller and Russell (2008, Ch. 148), Ketchum and Benson (2010, Ch. 174), Benson et al. (2012a, Ch. 180).

Elasmosaurus platyurus

Ch. 230 (**0**) S; (**?**) O'G.

As the specimens are not able to be revised in this type of features regarding outlines the scoring? is preferred.

232*. Anterior limb postaxial accessory ossicles contacting with humerus: absent, or small, round elements appearing late in ontogeny without well-defined articular surfaces (**0**); present as small elements (**1**); present as large, well-defined elements **contacting humerus** via well-defined articular surfaces, ossification of these elements is often late but their presence can be inferred by the presence of articular surfaces (**2**). Two elements articulating with humerus **(3).**

Modified from Sato (2002: Ch. 199) by restriction to anterior limb and contact with humerus. Modified from Benson et al. (2012a, Ch. 182). Modified from Druckenmiller and Russell (20082008, Ch. 137), Ketchum and Benson (2010, Ch.s 160–161) (merged separate Ch.s/states of the propodial and epipodial rows). Modified from O'Keefe (2001, Ch. 153), O'Keefe and Wahl (2003, Ch. 87), Albright et al. (2007, Ch. 20), O'Keefe (2008, Ch. 20), O'Keefe and Street (2009, Ch. 78).

Kawanectes lafquenianum

Ch. 232 (**?**) S; (**2**) O'G.

Based on personal observations of MLP 71-II-13-1.

Kaiwhekea katiki

Ch. 232 (**0**) S; (**2**) O'G.

Based on personal observations of OU 12649 (Fig. S6E).

Vegasaurus molyi

Ch. 232 (**?**) S; (**2**) O'G.

Based on personal observations of MLP 93-I-5-1.

233*. Second postaxial accessory ossicle (do not articulated with humerus): absent (**0**); present articulating with a wide notch between ulna and ulnare (**1**); **articulate only with ulna (2)**. **Modified** from Benson and Druckenmiller (2014) by restriction on element articulation and new state 2.

Kawanectes lafquenianum

Ch. 233 (**0**) S; (**?**) O'G.

Based on personal observation of hypodigm of O'Gorman, 2016b

Kaiwhekea katiki

Ch. 233 (**0**) S; (**?**) O'G.

Based on personal observations of OU 12649 (holotype).

Futabasaurus suzukii

Ch. 233 (**0**) S; (**1**) O'G.

Based on Sato et al., 2006:fig 2.

Hydrotherosaurus alexandrae

Ch. 233 (**0**) S; (**2**) O'G.

Based on personal observations of UCMP 33912 (Fig. S6F).

Vegasaurus molyi

Ch. 233 (**0**) S; (**?**) O'G.

Based on personal observation of MLP 93-I-5-1 (holotype).

Wapuskanectes betsynichollsae

Ch. 233 (**0**) S; (**?**) O'G

Based on personal observations of and Druckenmiller and Russelll (2006) and observation personal of TMP 98.49.02.

235. Fore fin, ratio of proximodistal length excluding humerus to maximum anteroposterior width of humerus/proximal epipodials [aspect ratio]: <3.0 (**0**); 3.1–3.5 (**1**); >3.6 (**2**). Modified from Druckenmiller and Russell (2008, Ch. 130), Ketchum and Benson (2010, Ch. 155): quantitative Chs describing the fore fin aspect ratio. Modified from O'Keefe (2001, Ch. 7), Sato (2002, Ch. 180), O'Keefe and Wahl (2003, Ch. 6), O'Keefe and Street (2009, Ch. 6).

Aristonectes quiriquinensis

Ch. 235 (**?**) S; (**2**) O'G

Based on Otero et al. (2014:fig. 15) and some estimation of the extension of the lost tip.

Callawayasaurus colombiensis

Ch. 235 (**?**) S; (**2**) O'G

Based on personal observation of RA4425, postcranium (Fig. S6G; 7A).

Morenosaurus stocki

Ch. 235 (**?**) S; (**2**) O'G

Based on Welles (1943:fig 19) and personal observation of LACM 2802.

239. Humerus, long axis curvature in anterior view: straight or almost straight (0); pronounced dorsodistal curve (1). Benson et al. (2012*a*, Ch. 185).

Wapuskanectes betsynichollsae

Ch. 239(**1**) S; (**?**) O'G

Based on personal observation of TMP 98.49.02.

"Speeton Clay Plesiosaurian"

Ch. 239(**1**) S; (**0**) O'G

Based on personal observation of SCARB200751 (on display).

240. Femur, long axis curvature in anterior view: straight or almost straight (**0**); pronounced dorsodistal curve (**1**); pronounced ventrodistal curve (**2**).

Benson et al. (2012a, Ch. 186).

Aristonectes quiriquinensis

Ch. 240 (**?**) S; (**0**) O'G

Based on Otero et al. (2014:fig. A, C).

Callawayasaurus colombiensis

Ch. 240 (**?**) S; (**0**) O'G

Based on personal observation of RA4425, (Bogota specimen of Welles, 1962).

244*. Humerus length *versus* width ratio: >2.9 (**0**); 2.3–2.7 (**1**); 1.7–2.2 (**2**); < 1.6-1,4 (3); < 1,4 (4) **New quantification**.

Modified from Bardet et al. (1999, Ch. 29), Sato (2002, Ch. 184), Druckenmiller and Russell (2008, Ch. 132), Smith and Dyke (2008, Ch. 87), Ketchum and Benson (2010, Ch. 154), Benson et al. (2012a, Ch. 244).

Vegasaurus molyi Ch. 244 (3) S; (**0**) O'G /***Kawanectes lafquenianum*** Ch. 244 (3) S; (**0**) O'G/***Kaiwhekea katiki*** Ch. 244 (3) S; (**0**) O'G/ ***Hydralmosaurus serpentinus*** Ch. 244 (3) S; (4) O'G/ ***Wapuskanectes betsynichollsae***/ Ch. 244 (3) S; (4) O'G. Modified based on personal observations and different quantification**.**

245. Preaxial margin of distal humerus in dorsal or ventral view: straight or convex (**0**); concave [distal humerus expands anteriorly], but anterior expansion relatively small, substantially less than posterior expansion (**1**); concave, and anterior expansion is large, approaching the size of the posterior expansion (**2**). Benson et al. (2012a, Ch. 188). Modified from O'Keefe (2001, Ch. 150), Sato (2002, Ch. 186), O'Keefe and Wahl (2003, Ch. 82), Druckenmiller and Russell (2008, Ch. 133), O'Keefe and Street (2009, Ch.73), Modified from Ketchum and Benson (2010, Ch.157), Vincent et al. (2011, Ch. 62); Smith and Dyke (2008, Ch. 89).

Albertonectes vanderveldei

Ch. 245 (**1**) S; (**2**) O'G

Based on personal observations of TMP 2007.011.0001 and Kubo et al., 2012:fig. 2012:fig. 8.

Aristonectes quiriquinensis

Ch. 245 (**2**) S; (**1**) O'G

Based on Otero et al., 2014:fig 15C, D.

Callawayasaurus colombiensis

Ch. 245 (**0**) S; (**1**) O'G

Based on (Welles, 1962 figs: 5a, 6a) and personal observation of UCPM 125328 (Fig. S7A). .

Hydrotherosaurus alexandrae

Ch. 245 (**1**) S; (**2**) O'G

Based on personal observations of UCMP 33912 holotype and only specimen (Fig. S7C).

Terminonatator ponteixensis

Ch. 245 (**1**) S; (**2**) O'G

Based on Sato (2003:fig. 13A, B).

Zarafasaura oceanis

Ch. 245 (**1**) S; (**2**) O'G

Based on Lomax and Wahl, 2013:fig. 11.

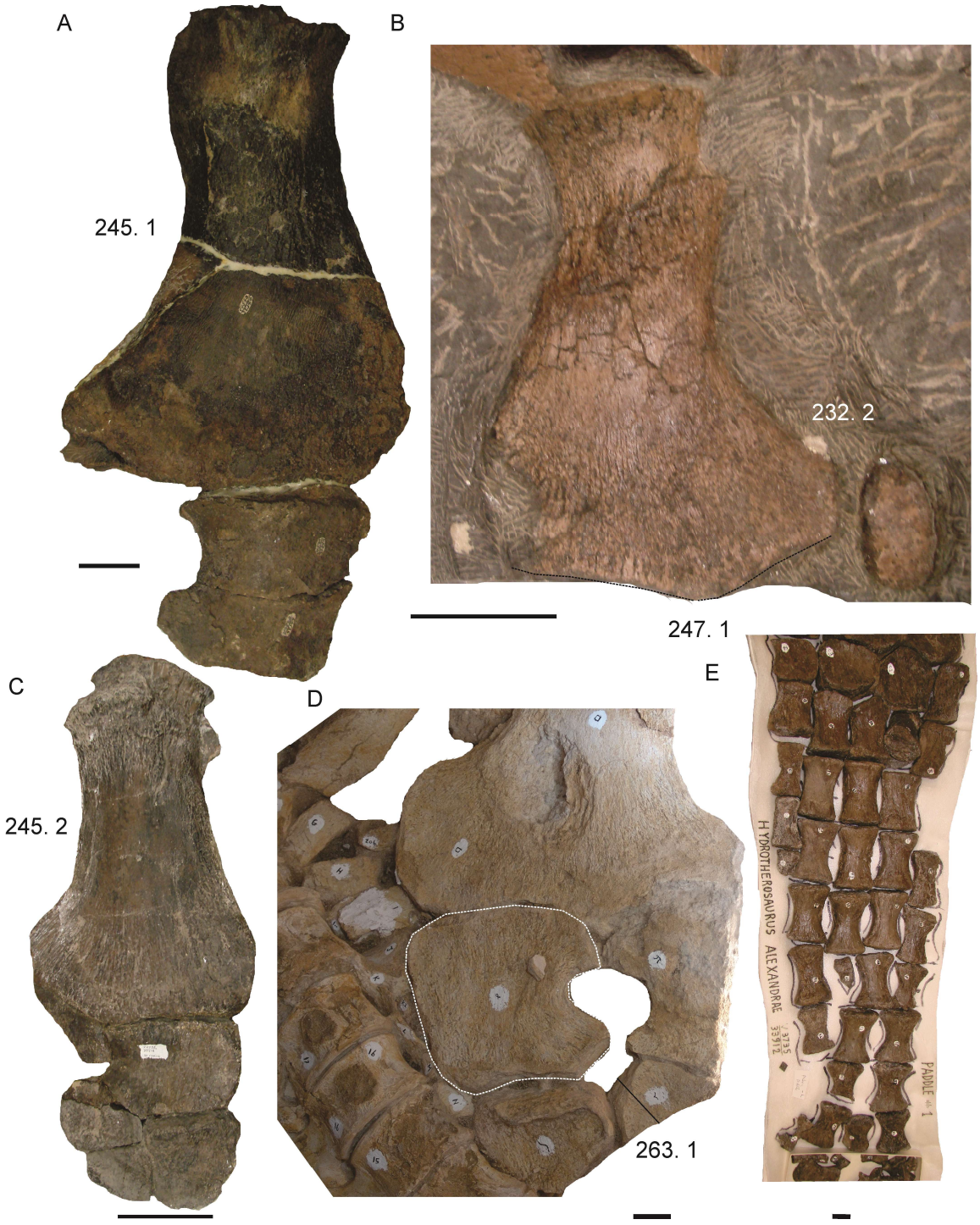

FIGURE S **S**7. **A**, *Callawayasaurus colombiensis* (RA4425, Bogotá specimen), right anterior limb in ventral view. Scale bar equals 50 mm. **B**, *Wapuskanectes betsynichollsae* (TMP 98.49.02, holotype), right humerus in ventral view. Scale bar equals 100 mm. **C**,

Hydrotherosaurus alexandrae (UCMP 33912, holotype), **D**, right anterior limb in dorsal view. *Zarafasaura oceanis* (WDC CMC-01, referred specimen), anterior right limb in ventral view. Scale bar equals 20 mm. **E**, *Hydrotherosaurus alexandrae* (UCMP 33912, holotype), left hind limb in ventral view. Scale bars equal 20 mm.

247. Shape of the distal end of propodials: uniformly convex (**0**); propodials distinctly angled for articulation with the epipodials (**1**). O'Keefe (2001, Ch. 152), O'Keefe and Wahl (2003, Ch. 83), Druckenmiller and Russell (2008, Ch. 136), Smith and Dyke (2008, Ch. 91), O'Keefe and Street (2009, Ch. 74), Ketchum and Benson (2010, Ch. 159), Benson et al. (2012a, Ch. 190).

Gronausaurus wegneri

Ch. 247 (**0**) S; (0/1) O'G

The scoring of this stated is not clear. See Hampe (2013:fig. 8).

Wapuskanectes betsynichollsae

Ch. 247 (**0**) S; (**1**) O'G

Based on personal observations on TMP 98.49.02 (Fig. S7B).

248. Humerus, angle between long axes of epipodial facets in dorsal view: oblique (**0**); close to 180° degrees (**1**). Sato (2002, Ch. 198).

Zarafasaura oceanis

Ch. 248 (**1**) S; (**0**) O'G

Based on Lomax and Wahal (2013:fig. 11A, B).

249. Humerus, inclination of proximal end in dorsal view: inclined posteriorly so that the proximal portion of the anterior margin is convex in dorsal view [often a low mound is located proximally on anterior surface] (**0**); not inclined, extends proximally so shaft appears straight (**1**); inclined anteriorly so shaft appears sigmoidal (**2**). Benson et al. (2012a, Ch. 191). State 1 from O'Keefe and Wahl (2003, Ch. 95), Albright et al. (2007, Ch. 18), O'Keefe (2008, Ch. 18), O'Keefe and Street (2009, Ch. 86). State 2 from Smith and Dyke (2008, Ch. 89).

Vegasaurus molyi, Ch. 249 (**1**) S; (**2**) O'G/***Kawanectes lafquenianum***; Ch. 249 (**1**) S (**2**) O'G/ ***Aristonectes quiriquinensis***, Ch. 249 (**1**) S; (**2**) O'G/***Kaiwhekea katiki,*** Ch. 249 (**1**) S; (**2**) O'G.

Based on personal observations of MLP 93-I-5-1; MLP 71-II-13-1; SGO PV 957; OU 12649 and O'Gorman, et al. (2015); O'Gorman, (2016a) and Otero et al. (2014).

However this character is extremely subjective as the proximal inclination of humerus is usually difficult to assess.

Albertonectes vanderveldei

249 (**1**) S; (**2**) O'G.

Based on Kubo et al., 2012:fig.8A.

Hydrotherosaurus alexandrae

249 (**1**) S; (**2**) O'G.

Based on personal observation of UCMP 33912 (Fig. S7C)

Terminonatator ponteixensis

249 (**1**) S; (**2**) O'G.

Based on Sato (2003:fig.13B).

Zarafasaura oceanis

249 (**1**) S; (**2**) O'G.

Based on Based on Lomax and Wahal (2013:fig. 11A, B).

252. Humerus, tuberosity morphology: narrow and projects dorsally (**0**); broad and projects posterodorsally [tilted] (**1**). Sato (2002, Ch. 192).

Brancasaurus brancai

Ch. 252 (**0**) S; (**1**) O'G

Based on Hampe (2013:fig. 8b) and Sachs and Ker (2016:21A).

253*. Femur, trochanter morphology: extends slightly dorsally (0); more extended dorsally and in diagonal direction (1).

Modified from Benson and Druckenmiller (2014, Ch. 253); O'Gorman (2016b: Ch. 271); Sato (2002, Ch. 193).

Scoring modified following this modification.

254. Ratio of radius length to maximum width: >2.7 (0); 1.1–1.5 (1); 0.8–1.0 (2); < or equal to 0.75 (3). Modified from Smith and Dyke (2008, Ch. 93), Ketchum and Benson (2010, Ch. 162), Benson *et al.* (2012*a*, Ch. 194). Modified from Sato (2002, Ch. 202), Druckenmiller and Russell (2008*a*, Ch. 138), Vincent *et al.* (2011, Ch. 64) , O'Keefe (2001, Ch. 161), O'Keefe and Wahl (2003*b*, Ch. 86), Albright *et al.* (2007*b*, Ch. 21), O'Keefe (2008, Ch. 21), O'Keefe and Street (2009, Ch. 77) (epipodial proportions).

Gronausaurus wegneri

Ch. 254 (**?**) S; (**2**) O'G

Based on Hampe, 2013.

255. Ratio of tibia length to maximum width: >2.5 (**0**); 1.–1.8 (**1**); <1 (**2**). Modified from Ketchum and Benson (2010, Ch. 177), Benson et al. (2012a, Ch. 195) (different quantifications). Modified from Sato (2002, Ch. 203), Druckenmiller and Russell (2008, Ch. 151), Vincent et al. (2011, Ch. 66) (tibia and fibula). Modified from O'Keefe (2001, Ch. 161), O'Keefe and Wahl (2003, Ch. 86), Albright et al. (2007, Ch. 21), O'Keefe (2008, Ch. 21), O'Keefe and Street (2009, Ch. 77) (epipodial proportions).

Based different quantification all "3" where scored as "2" to avoid oversatated minor differences in tibia proportions.

Aristonectes quiriquinensis

Ch. 255 (**?**) S; (**1**) O'G

Based on Otero et al., 2014:fig. 15C, D.

Callawayasaurus colombiensis

Ch. 255 (**2**) S; (**1**) O'G

Based on personal observations of the ("Bogotá specimen" of Welles, 1962: RA4425).

Gronausaurus wegneri

Ch. 255 (**1**) S; (**?**) O'G

Based on the absence of well preserved tibia in *G. wegneri* holotype (Hampe, 2013)

Zarafasaura oceanis

Ch. 255(**2**) S; (**1**) O'G

Based on Lomax and Wahal, 2013:fig. 13.

Hydrotherosaurus alexandrae

Ch. 255(**2**) S; (**1**) O'G

Based on personal observation of UCMP 33912

Kawanectes lafquenianum

Ch. 255(**?**) S; (**1**) O'G

Based on personal observation of MCS PV 4.

256. Radius morphology: preaxial margin concave (**0**); straight or convex (**1**).

Ketchum and Benson (2010, Ch. 163), Benson et al. (2012a, Ch. 196).

Modified from O'Keefe and Street (2009, Ch. 90) (radius). Modified from Sato (2002, Ch. 204), Druckenmiller and Russell (2008, Ch. 139), Vincent et al. (2011, Ch. 65) (radius and ulna).

Gronausaurus wegneri

Ch. 256 (**?**) S; (**1**) O'G

Based on Hampe, 2013.

Hydrotherosaurus alexandrae

Ch. 256 (**0**) S; (**1**) O'G

Based on personal observation of UCMP 33912 (Fig. S7C).

Callawayasaurus colombiensis

Ch. 256 (**0**) S; (**1**) O'G

Based on personal observations of UCPM 38349 and RA4425 (Fig. S7A).

259. Tibia morphology: preaxial side of tibia concave (**0**); convex or straight (**1**).

Benson et al. (2012a, Ch. 199). Modified from Sato (2002, Ch. 205), Druckenmiller and Russell (2008, Ch. 152), Vincent et al. (2011, Ch. 67) (tibia and fibula).

Kaiwhekea katiki

Ch. 259 (**0**) S; (**?**) O'G

Based on personal observation of OU 12649, the margin seems to be damage.

Vegasaurus molyi

Ch. 259 (**0**) S; (**?**) O'G

Based on personal observation of the MLP 93-III-3-1, this area is affected by deformation so it is not sure the scoring.

Zarafasaura oceanis

Ch. 259 (**?**) S; (**1**) O'G

Based on Lomax and Wahal (2013:fig. 13).

263*. Radius, posterodistal facet for intermedium: absent (**0**); present and well developed at least the half of the length of the ulnar facet for intermedium (**1**); **reduced (2)**. Modified from Benson et al. (2012a, Ch. 203) by adding state 2.

Aristonectes quiriquinensis

Ch. 263 (**1**) S; (**2**) O'G

Otero et al., 2014:fig. 16.

Zarafasaura oceanis

Ch. 261 (**0**) S; (**1**) O'G

See Fig. S7D.

264. Tibia, posterodistal facet for intermedium: absent (**0**); present and well developed at least the half of the length of the ulnar facet for intermedium (**1**); reduced (**2**). Modfied from Benson and Druckenmiller, 2014 by addition of state 2. Ketchum and Benson (2011*a*, Ch. 200). Benson et al. (2012a, Ch. 204).

Aristonectes quiriquinensis

Ch. 264 (**1**) S; (**2**) O'G

Based on Otero et al., 2014:fig. 16.

265. Width of epipodials of the hindlimb: tibia larger (**0**); widths within 10% of each other (**1**); fibula larger (**2**).

Modified from Sato (2002, Ch. 197).

Kaiwhekea katiki

Ch. 265 (**2**) S; (**?**) O'G

Based on personal observations, the tibia is not well preserved and therefore this could not be scored with certainty.

270. Phalanx proportions: long and slender [~2-3 times as long proximodistally as broad anteroposteriorly] (**0**); short and robust (**1**).

Benson et al. (2012a, Ch. 207).

Callawayasaurus colombiensis

Ch. 270 (**1**) S; (**0**) O'G

Based on personal observation of the RA4425.

Hydrotherosaurus alexandrae

Ch. 270 (**1**) S; (**0**) O'G

Based on personal observation of UCMP 33912 (Fig. S7E).

Kawanectes lafquenianum

Ch. 270 (**1**) S; (**?**) O'G.

No available material is preserved to be sure. Only one phalange is figured O'Gorman, (2016) and it is severely deformed.

Zarafasaura oceanis

Ch. 270 (**?**) S; (**0**) O'G

Based on Lomax and Wahl (2013:fig: 13).

Characters added to the data set of Benson and Druckenmiller (2014) and Serratos et al. (2017).

271. Contact pterygoid with quadrate. Trough a long process (**0**); trough a wide "plate like" process, (**1**).

Modified from Otero et al. (2016), see SF 8A-C.

This character cover the morphologies observed on the quadrate ramus of pterygoid observed among elasmosaurids that shows a stick like morphology such as in *Libonectes morgani* or *Callawayasaurus colombiensis* (O'Gorman et al., 2018) or a plate-like morphology as in *Aristonectes quiriquinensis* or *Alexandornectes zealandiensis* (O'Gorman et al., 2018).

272. Procumbent teeth in premaxilla, maxilla and mandible: Absent (**0**); Present (**1**).

Gasparini et al. (2003); Otero et al. (2014).

Although some grade or lateral direction is present in all plesiosaurians and particularly elasmosaurids the scoring "1" was given for those that all the alveoli periphery is visible in

lateral view (See O′Gorman, 2016:Fig. 2) and this condition is present in premaxilla, maxilla and dentary as in *Aristonectes quiriquinensis* and *Morturneria seymourensis*.

273. Vomer anterior end. Convex (**0**); With a medial concavity or two lateral concavities (**1**). The vomer shows an anterior end convex as in *Libonectes morgani* or *Tuarangisaurus keyesi* (Carpenter, 1996; O'Gorman et al., 2017) or shows a medial or two lateral concave margins as in *Futabasaurus suzukii* or *Aristonectes parvidens* (Sato et al., 2006; Gasparini et al., 2003).

New Character.

274. Mandible 100*wide/length: < 60, (**0**); > 60, (**1**).

New Character.

This character considered the proportions of the mandible scoring as, independently of its bowed condition.

275. Subdiapophyseal fossa: absent (**0**); present (**1**).

Hampe, 2013

Hampe defined the subdiapophyseal fossa as a deep concavity below the diapophysis of dorsal vertebrae. Here only those specimens where the author or detailed descriptions indicate its present were scored as (1). It seems to be absent in al l the revised elasmosaurids.

276. Clavicle-interclavicle complex medial ventral keel: absent (**0**); present (**1**).

Sato (2002 Ch. 154).

277. Clavicle-interclavicle complex marked posterior medial embayment: present (**0**); Absent (**1**).

New Character.

This character take the variability of the posterior margin of the clavicle-interclavicle complex. Indicating if it shows a medial embayment such as in *Futabasaurus suzukii*, *Thalassomedon haningtoni* and *Callawayasaurus colombiensis* (Fig. 10)

278. Clavicle-interclavicle complex posterior process: absent (**0**); present (**1**)

O′Keefe (2001 Ch. 131); Ketchum and Benson (2010; Ch. 140).

279. Clavicle-interclavicle complex shape: triangular (**0**); rectangular (**1**).

Modified from Rieppel (1994 Ch. 61); Druckenmiller and Russell (2008 Ch. 121).

This character cover the rough shape of the clavicle-interclavicle complex between triangular and subrectangular, been scored as "**1**" only *Aphrosaurus furlongi* and MLP 99-XII-1-5.

280. Dorsal sector of ilium (dorsal to the bend point): longer than ventral (**0**): equal to ventral (**1**). Inapplicable (**?**) not divided into dorsal and ventral sectors. Modified from Smith and Dyke (2008 Ch. 85) with differentiation of dorsal and ventral parts.

281. Dorsal sector of ilium (dorsal to the bend point): more gracile than ventral (**0**): equal to ventral (**1**). Inapplicable (**?**) not divided into dorsal and ventral sectors. Modified from Smith and Dyke (2008 Ch. 85).

282. Ventral surface of the humerus, deep depression anterior to the main muscle scar: absent (**0**) present (**1**). O'Gorman and Coria (2016 Ch.274).

The anterior depression is a well-developed depression anterior to the main ventral muscle scar. It seems to be well developed in *Vegasaurus molyi*, *Kawanectes lafquenianum* and *Aphrosaurus furlongi* but absent in other elasmosaurids (O′Gorman and Coria, 2017).

283: Humerus ulnar expansion: absent or small (**0**); developed (**1**).

Sato, 2002 ch. 187.

The humerus ulnar expansion (Sato, 2003) or "posterior expansion" (O′Gorman et al., 2015) is a posterior extension in the distal expansion of humerus. It generates a deep concavity in the posterior margin of humerus in dorsal or ventral view. Here only the species where the expansion is well defined are scores as (1).

FIGURE S8. Character 271. Posterior palate in ventral view **A**, (UCPM 125328, *Callawayasaurus colombiensis*) and **B** (SMUSMP 69120, *Libonectes morgani*) =Ch. 271.0; **C** (CM Zfr 91, *Alexandronectes zealandiensis*) =Ch. 271.1. MLP 99-XII-1-5. Aristonectinae indet. **D**–**E**, cervical vertebrae in **D**, anterior and **E**, ventral views. **F**–I,

clavicle-interclavicle complex in **F**, dorsal, **H**, ventral, **H**, anterior and **I**, posterior views. Scale bars equal 20 mm.

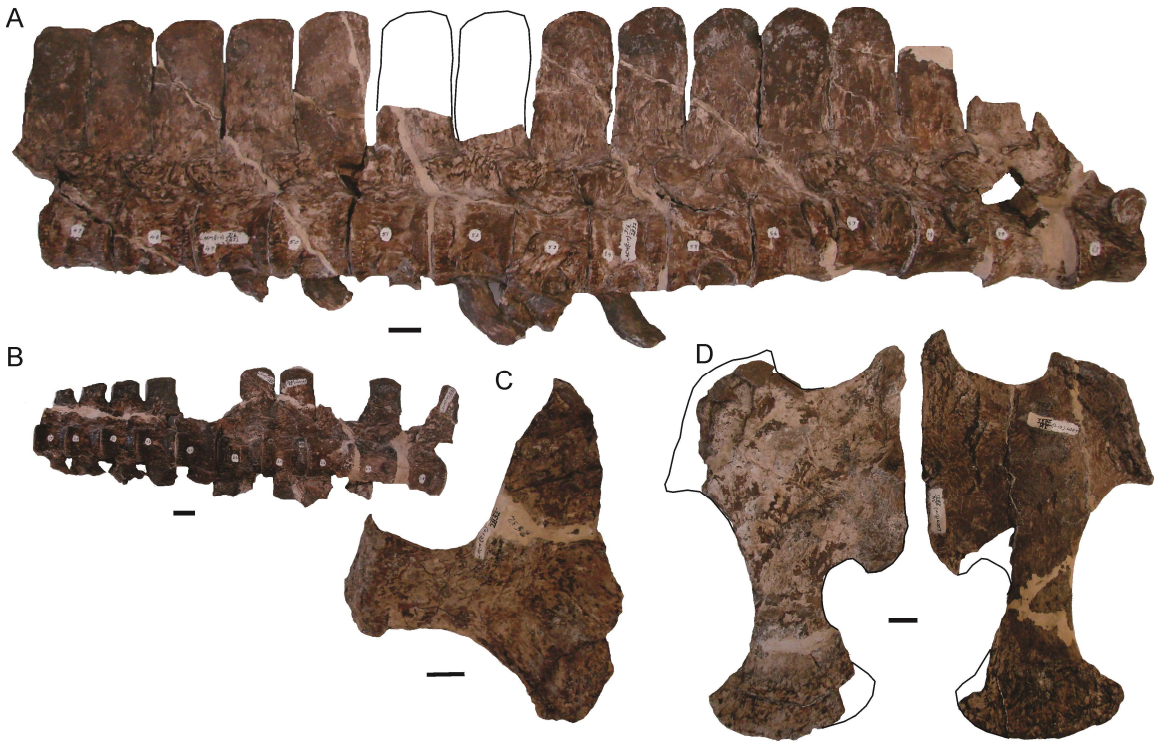

FIGURE S9. Elasmosauridae indet. LACM 2832. **A**, Posterior cervical, pectorals and first two dorsal vertebrae in left lateral view. **B**, Anterior middle cervical vertebrae in left lateral view. **C**, left scapula in dorsal view. **D**, Coracoid in ventral view. Scale bar = 20 mm.

ACKNOWLEDGMENTS

This research was supported by projects PICT 2015-0678. I thank Z. Gasparini (UNLP) and L. Salgado (UNRN) for reading an earlier version of this manuscript, and the curators of the reviewed collections for providing access to the material; ANSP (N. Gilmore) CM, (P.

Scofield); Dorchester Museum (P. Tomlinson); LACM (M. Walsh); MCS (I. Cerda); MLP (M. Reguero); MML (D. Cabaza); MPEF (E. Ruigomez); TMP (D. Brinkman); MANH (M. Norell); Manchester Museum (D. Gelsthorpe); MCZ, (J. Cundiff); MIWG (M. Munt); Museum of New Zealand Te Papa Tongarewa (A.J.D., Tennyson); OU (E. Fordyce). OXFUM (H. Ketchum); Peterborough Museum & Art Gallery (G. Wass); Segdwich Museum (M. Riley); UCPM (P. Holroy); Yorkshire Museum (S. King). The author also thanks D. Lomax and B. Wahl (Wyoming Dinosaur Center) for providing photographyc material of the specimen WDC CMC-01. The author thank the Willi Hennig Society for the access to the TNT free software. The authors thank two anonymous reviewers for the comments that improve this contribution.

LITERATURE CITED

Allemand, R., N. Bardet, A. Houssaye, and P. Vincent. 2017. Virtual reexamination of a plesiosaurian specimen (Reptilia, Plesiosauria) from the Late Cretaceous (Turonian) of Goulmima, Morocco, using computed tomography. Journal of Vertebrate Paleontology. DOI: 10.1080/02724634.2017.1325894.

Albright, L. B. III, D. D. Gillette, and A. L. Titus. 2007. Plesiosaurs from the Upper cretaceous (Cenomanian–Turonian) Tropic Shale of southern Utah, part 2: Polycotylidae. Journal of Vertebrate Paleontology 27: 41–58.

Bardet, N., P. Godefroit, and J. Sciau. 1999. A new elasmosaurid plesiosaur from the Lower Jurassic of southern France. Palaeontology 42:927–952.

Benson, R. B., and P. S. Druckenmiller. 2014. Faunal turnover of marine tetrapods during the J urassic–C retaceous transition. Biological Reviews 89: 1–23.

Benson, R. B. J., K. T. Bates, M. R. Johnson, and P. J. Withers. 2011*a*. Cranial anatomy of *Thalassiodracon hawkinsi* (Reptilia, Plesiosauria) from the Early Jurassic of Somerset, United Kingdom. Journal of Vertebrate Paleontology 31:562–574.

Benson, R. B. J., M. Evans, and P. S. Druckenmiller. 2012a. High diversity, low disparity and small body size in plesiosaurs (Reptilia, Sauropterygia) from the Triassic-Jurassic boundary. PLoS ONE 7:e31838.

Benson, R. B. J., H.F. Ketchum, D. Naish, and L. E. Turner. 2012b. A new leptocleidid (Sauropterygia, Plesiosauria) from the Vectis Formation (early Barremian–early Aptian; Early Cretaceous) of the Isle of Wight and the evolution of Leptocleididae, a controversial clade. Journal of Systematic Palaeontology 11:233–250.

Benson, R. B. J., H.F. Ketchum, L. F. Noé, and M. Gómez-Pérez. 2011b. New information on *Hauffiosaurus* (Reptilia, Plesiosauria) based on a new species from the Alum Shale Member (lower Toarcian: Lower Jurassic) of Yorkshire, UK. Palaeontology 54:547–571.

Carpenter, K. 1997. Comparative cranial anatomy of two North American Cretaceous plesiosaurs. In: Callaway, J.M., Nicholls, E.L. (Eds.). Ancient marine reptiles. Academic Press, San Diego, 191–216.

Carpenter, K. 1999. Revision of North American elasmosaurs from the Cretaceous of the Western Interior. Paludicola 2:148–173.

Cabrera, A. 1941. Un plesiosaurio nuevo del Cretaceo del Chubut. Revista del Museo de La Plata 2:113–130.

Cruickshank, A. R., and R. E. Fordyce. 2002. A new marine reptile (Sauropterygia) from New Zealand: further evidence for a Late Cretaceous austral radiation of cryptoclidid plesiosaurs. Palaeontology, 45: 557–575.

Druckenmiller, P. S., and A. P Russell. 2006. A new elasmosaurid plesiosaur (Reptilia: Sauropterygia) from the Lower Cretaceous Clearwater Formation, northeastern Alberta, Canada. Paludicola 5: 184–199.

Druckenmiller, P. S., and A. P. Russell. 2008. A phylogeny of Plesiosauria (Sauropterygia) and its bearing on the systematic status of *Leptocleidus* Andrews, 1922. Zootaxa 1863:1–120.

Gasparini, Z., N. Bardet, and M. Iturralde-Vinent. 2002. A new cryptoclidid plesiosaur from the Oxfordian (Late Jurassic) of Cuba. Geobios 35:201–211.

Gasparini, Z., J. E. Martin, and M. Fernández. 2003. The elasmosaurid plesiosaur *Aristonectes* Cabrera from the Latest Cretaceous of South America and Antarctica. Journal of Vertebrate Paleontology 23:104–115.

Großmann, F. 2007. The taxonomic and phylogenetic position of the Plesiosauroidea from the Lower Jurassic Posidonia Shale of south-west Germany. Palaeontology 50:545–564.

Hampe, O. 2013. The forgotten remains of a leptocleidid plesiosaur (Sauropterygia: Plesiosauroidea) from the Early Cretaceous of Gronau (Münsterland, Westphalia, Germany). Paläontologische Zeitschrift 87:473-491.

Hiller, N., A. A. Mannering, C.M. Jones, and A. R., Cruickshank. 2005. The nature of *Mauisaurus haasti* Hector, 1874 (Reptilia: Plesiosauria). Journal of Vertebrate Paleontology 25:588–601.

Hiller, N., J. P. O'Gorman, R. A. Otero, and A. A. Mannering. 2017. A reappraisal of the Late Cretaceous Weddellian plesiosaur genus *Mauisaurus* Hector, 1874. New Zealand Journal of Geology and Geophysics 60:112–128.

Kear, B. P. 2005. A new elasmosaurid plesiosaur from the Lower Cretaceous of Queensland, Australia. Journal of Vertebrate Paleontology 25, 792–805.

Kear, B. P. 2007. Taxonomic clarification of the Australian elasmosaurid genus *Eromangasaurus*, with reference to other austral elasmosaur taxa. Journal of Vertebrate Paleontology 27:241–246

Ketchum, H. F. and R. B. Benson. 2010. Global interrelationships of Plesiosauria (Reptilia, Sauropterygia) and the pivotal role of taxon sampling in determining the outcome of phylogenetic analyses. Biological Reviews 85:361–392.

Ketchum, H. F. and R. B. J. Benson. 2011. A new pliosaurid (Sauropterygia, Plesiosauria) from the Oxford Clay Formation (Middle Jurassic, Callovian) of England: evidence for a gracile, longirostrine grade of Early–Middle Jurassic pliosaurids. Special Papers in Palaeontology 86:109–129.

Lomax, D. R. and W. Wahl. 2013. A new specimen of the elasosaurid plesiosaur *Zarafasaura oceanis* from the Upper Cretaceous (Maastrichtian) of Morocco. Paludicola 9: 97–109.

O'Keefe, F. R. 2001. A cladistic analysis and taxonomic revision of the Plesiosauria (Reptilia: Sauropterygia). Acta Zoologica Fennica 213:1–63.

O'Keefe, F. R. 2004a. Preliminary description and phylogenetic position of a new plesiosaur (Reptilia: Sauropterygia) from the Toarcian of Holsmaden, Germany. Journal of Paleontology 78:973–988.

O'Keefe, F. R. 2004b. On the cranial anatomy of the polycotylid plesiosaurs, including new material of *Polycotylus latipinnis*, Cope, from Alabama. Journal of Vertebrate Paleontology 24:326–340.

O'Keefe, F. R. 2008. Cranial anatomy and taxonomy of *Dolichorhynchops bonneri* new combination, a polycotylid (Sauropterygia: Plesiosauria) from the Pierre Shale of Wyoming and South Dakota. Journal of Vertebrate Paleontology 28:664–676.

O'Keefe, F. R., and N. Hiller. 2006. Morphologic and ontogenetic patterns in elasmosaur neck length, with comments on the taxonomic utility of neck length variables. Paludicola 5:206–229.

O'Keefe, F. R., and H. P. Street. 2009. Osteology of the cryptocleidoid plesiosaur *Tatenectes laramiensis*, with comments on the taxonomic status of the Cimoliasauridae. Journal of Vertebrate Paleontology 29:48–57.

O'Keefe, F. R., and W. Wahl. 2003. Preliminary report on the cranial osteology and relationships of a new cryptocleidoid plesiosaur from the Sundance Formation, Wyoming. Paludicola 4:48–68.

O'Gorman, J. P. 2016a. New insights on the Aristonectes parvidens (Plesiosauria, Elasmosauridae) holotype: News on an old specimen. Ameghiniana 53:397–417.

O'Gorman, J. P. 2016b. A small body sized non-aristonectine elasmosaurid (Sauropterygia, Plesiosauria) from the Late Cretaceous of Patagonia with comments on the relationships of the Patagonian and Antarctic elasmosaurids. Ameghiniana 53:245–268.

O'Gorman, J. P. 2017. First record of *Kawanectes lafquenianum* (Elasmosauridae, Sauropterygia) from la Colonia Formation, Chubut. 31 JAPV, Santa Clara del Mar, Argentina. Abstracts: 44.

O'Gorman, J. P., and R. A. Coria 2017. A new elasmosaurid specimen from the upper Maastrichtian of Antarctica: new evidence of a monophyletic group of Weddellian elasmosaurids. Alcheringa: An Australasian Journal of Palaeontology 41:240–249.

O'Gorman, J. P., R. A. Otero, N., Hiller, J., Simes, and M. Terezow. 2017. Redescription of *Tuarangisaurus keyesi* (Sauropterygia; Elasmosauridae), a key species from the uppermost Cretaceous of the Weddellian Province: Internal skull anatomy and phylogenetic position. Cretaceous Research 71:118–136.

O'Gorman, J. P., L., Salgado, E. B., Olivero, and S. A Marenssi. 2015a. *Vegasaurus molyi*, gen. et sp. nov.(Plesiosauria, Elasmosauridae), from the Cape Lamb Member (lower Maastrichtian) of the Snow Hill Island Formation, Vega Island, Antarctica, and remarks on Wedellian Elasmosauridae. Journal of Vertebrate Paleontology 35:e931285.

O'Gorman, J. P., R. A. Coria, M. Reguero, S. Santillana, T. Mörs, and M. Cárdenas 2018. The first non-aristonectine elasmosaurid (Sauropterygia; Plesiosauria) cranial material from Antarctica: New data on the evolution of the elasmosaurid basicranium and palate. Cretaceous Research 89: 248–263.

Otero, R. A. 2016. Taxonomic reassessment of *Hydralmosaurus* as *Styxosaurus*: new insights on the elasmosaurid neck evolution throughout the Cretaceous. PeerJ, 4, e1777.

Otero, R. A., S. Soto-Acuña, and D. Rubilar-Rogers. 2012. A postcranial skeleton of an elasmosaurid plesiosaur from the Maastrichtian of central Chile, with comments on the affinities of Late Cretaceous plesiosauroids from the Weddellian Biogeographic Province. Cretaceous Research 37: 89–99.

Otero, R. A., S. Soto-Acuña, and F. R. O'Keefe. 2018. Osteology of *Aristonectes quiriquinensis* (Elasmosauridae, Aristonectinae) from the upper Maastrichtian of central Chile. Journal of Vertebrate Paleontology 38, e1408638.

Otero, R. A., J. P., O'Gorman, N., Hiller, F. R., O'Keefe, and R. E. Fordyce. 2016. *Alexandronectes zealandiensis* gen. et sp. nov., a new aristonectine plesiosaur from the lower Maastrichtian of New Zealand. Journal of Vertebrate Paleontology 36:e1054494.

Otero, R. A., S., Soto-Acuña, F. R., O'Keefe, J. P., O'Gorman, W., Stinnesbeck, M. A., Suárez, D., Rubilar-Rogers, L. A., Quinzio-Sinn, and C.Salazar. 2014. *Aristonectes quiriquinensis* sp. nov., a new highly derived elasmosaurid from the late Maastrichtian of central Chile. Journal of Vertebrate Paleontology 34:100–125.

Rieppel, O. 1994. Osteology of *Simosaurus gaillardoti* and the relationships of stem group Sauropterygia. Fieldiana Geology, new series 28:1–85.

Sachs, S. and B. P. Kear. 2015. Postcranium of the paradigm elasmosaurid plesiosaurian *Libonectes morgani* (Welles, 1949). Geological Magazine 152:694–710.

Sachs, S. and B. P Kear. 2017. Redescription of the elasmosaurid plesiosaurian *Libonectes atlasense* from the Upper Cretaceous of Morocco. Cretaceous Research 74:205–222.

Sato, T. 2002. Description of plesiosaurs (Reptilia: Sauropterygia) from the Bearpaw Formation (Campanian–Maastrichtian) and a phylogenetic analysis of the Elasmosauridae. Ph.D. dissertation, University of Calgary, Calgary, Alberta, Canada, 391 pp.

Sato, T. 2003. *Terminonatator ponteixensis*, a new elasmosaur (Reptilia; Sauropterygia) from the Upper Cretaceous of Saskatchewan. Journal of Vertebrate Paleontology 23: 89–103.

Sato, T., Y. Hasegawa, and M. Manabe. 2006. A new elasmosaurid plesiosaur from the Upper Cretaceous of Fukushima, Japan. Palaeontology 49:467–484.

Seeley, H. G. 1874. Note on some of the generic modifications of the plesiosaurian pectoral arch. Quarterly Journal of the Geological Society 30: 436–449.

Serratos, D. J., P. Druckenmiller, and Benson, R. B. 2017. A new elasmosaurid (Sauropterygia, Plesiosauria) from the Bearpaw Shale (Late Cretaceous, Maastrichtian) of Montana demonstrates multiple evolutionary reductions of neck length within Elasmosauridae. Journal of Vertebrate Paleontology, e1278608.

Smith, A. S., and G. J. Dyke. 2008. The skull of the giant predatory pliosaur *Rhomaleosaurus cramptoni*: implications for plesiosaur phylogenetics. Naturwissenschaften 95:975–980.

Vincent, P., N., Bardet, X. P., Suberbiola, B., Bouya, M., Amaghzaz, and S. Meslouh. 2011. *Zarafasaura oceanis*, a new elasmosaurid (Reptilia: Sauropterygia) from the Maastrichtian Phosphates of Morocco and the palaeobiogeography of latest Cretaceous plesiosaurs. Gondwana Research 19:1062–1073.

Welles, S. P. and D. R. Gregg. 1971. Late Cretaceous marine reptiles of New Zealand. Records of the Canterbury Museum. 9:1–111.

Welles, S. P. 1943. Elasmosaurid plesiosaurs with description of new material from California and Colorado. Memoirs of the University of California 13:125–254.

Welles, S. P. 1962. A new species of elasmosaur from the Aptian of Colombia and a review of Cretaceous plesiosaurs. University of California Publications in Geological Sciences, University of California Berkeley 44:1–96.